Journal Pre-proof

Synergistic $PM_{2.5}$ and O_3 control to address the emerging global $PM_{2.5}$-O_3 compound pollution challenges

Chao He, Jianhua Liu, Yiqi Zhou, Jingwei Zhou, Lu Zhang, Yifei Wang, Lu Liu, Sha Peng

PII: S2772-9850(24)00032-2

DOI: https://doi.org/10.1016/j.eehl.2024.04.004

Reference: EEHL 102

To appear in: *Eco-Environment & Health*

Received Date: 14 January 2024

Revised Date: 5 March 2024

Accepted Date: 2 April 2024

Please cite this article as: C. He, J. Liu, Y. Zhou, J. Zhou, L. Zhang, Y. Wang, L. Liu, S. Peng, Synergistic $PM_{2.5}$ and O_3 control to address the emerging global $PM_{2.5}$-O_3 compound pollution challenges, *Eco-Environment & Health*, https://doi.org/10.1016/j.eehl.2024.04.004.

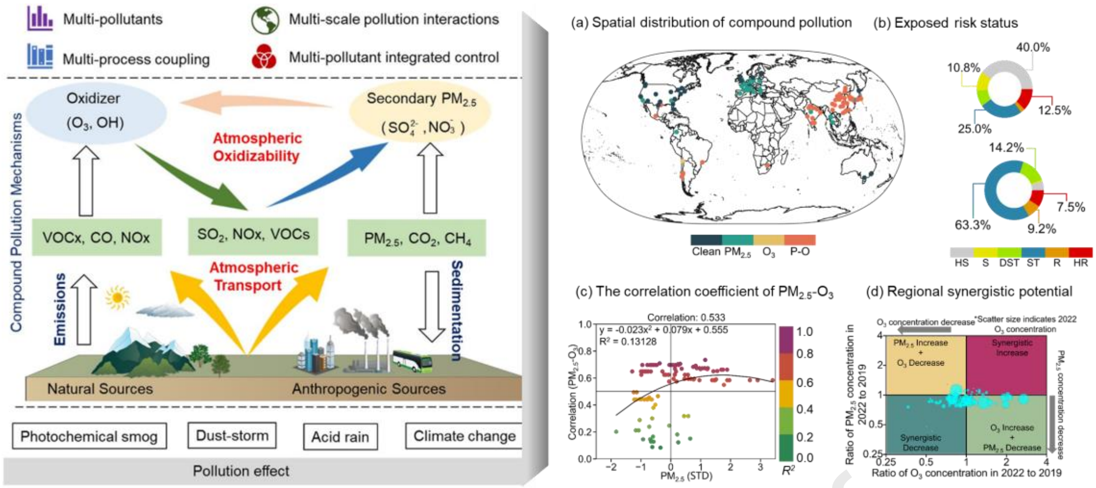

Multi-pollutants
Multi-scale pollution interactions
Multi-process coupling
Multi-pollutant integrated control
Oxidizer
(O_3, OH)
Secondary $PM_{2.5}$
(SO_4^{2-}, NO_3^-)
Atmospheric Oxidizability
VOCx, CO, NOx
SO_2, NOx, VOCs
$PM_{2.5}$, CO_2, CH_4
Atmospheric Transport
Compound Pollution Mechanisms
Emissions
Sedimentation
Natural Sources
Anthropogenic Sources
Photochemical smog
Dust-storm
Acid rain
Climate change
Pollution effect
(a) Spatial distribution of compound pollution
Clean $PM_{2.5}$ O_3 P-O
(b) Exposed risk status
40.0%
10.8%
12.5%
25.0%
14.2%
7.5%
63.3%
9.2%
HS S DST ST R HR
(c) The correlation coefficient of $PM_{2.5}$-O_3
Correlation: 0.533
y = -0.023x² + 0.079x + 0.555
R² = 0.13128
Correlation ($PM_{2.5}$-O_3)
$PM_{2.5}$ (STD)
R^2
(d) Regional synergistic potential
O_3 concentration decrease
*Scatter size indicates 2022 O_3 concentration
$PM_{2.5}$ Increase + O_3 Decrease
Synergistic Increase
Synergistic Decrease
O_3 Increase + $PM_{2.5}$ Decrease
Ratio of $PM_{2.5}$ concentration in 2022 to 2019
Ratio of O_3 concentration in 2022 to 2019
$PM_{2.5}$ concentration decrease

Synergistic $PM_{2.5}$ and O_3 control to address the emerging global $PM_{2.5}$-O_3 compound pollution challenges

Chao He[a,b,1,*] Jianhua Liu[a,b,1], Yiqi Zhou[c], Jingwei Zhou[d], Lu Zhang[e], Yifei Wang[f], Lu Liu[g*], Sha Peng[h*]

[a] College of Resources and Environment, Yangtze University, Wuhan 430100, China;

[b] Hubei Key Laboratory of Petroleum Geochemistry and Environment, Yangtze University, Wuhan 430100, China;

[c] School of Geography and Ocean Science, Nanjing University, Nanjing 210023, China;

[d] Hydrology and Environmental Hydraulics Group, Wageningen University and Research, Wageningen 6700 HB, The Netherlands;

[e] State Key Laboratory of Freshwater Ecology and Biotechnology, Institute of Hydrobiology, Chinese Academy of Sciences, Wuhan 430072, China;

[f] State Key Joint Laboratory for Environmental Simulation and Pollution Control, School of Environmental Sciences and Engineering, Peking University, Beijing 100871, China;

[g] State Key Laboratory of Pollution Control and Resource Reuse, School of Environment, Nanjing University, Nanjing 210023, China;

[h] Collaborative Innovation Center for Emissions Trading system Co-constructed by the Province and Ministry, Hubei University of Economics, Wuhan 430205, China;

[1] Co–first authors.

[*]Corresponding authors

E–mail address: hechao@yangtzeu.edu.cn (C. He); luliu@smail.nju.edu.cn (L. Liu); pengsha@hbue.edu.cn (S. Peng)

Abstract: In recent years, the issue of $PM_{2.5}$-O_3 compound pollution has become a significant global environmental concern. This study examines the spatial and temporal patterns of global $PM_{2.5}$-O_3 compound pollution and exposure risks, firstly at the global and urban scale, using spatial statistical regression, exposure risk assessment, and trend analyses based on the datasets of daily $PM_{2.5}$ and surface O_3 concentrations monitored in 120 cities around the world from 2019 to 2022. Additionally, on the basis of the common emission sources, spatial heterogeneity, interacting chemical mechanisms, and synergistic exposure risk levels between $PM_{2.5}$ and O_3 pollution, we proposed a synergistic $PM_{2.5}$-O_3 control framework for the joint control of $PM_{2.5}$ and O_3. The results indicated that: (1) Nearly 50% of cities worldwide were affected by $PM_{2.5}$-O_3 compound pollution, with China, Korea, Japan, and India being the global hotspots for $PM_{2.5}$-O_3 compound pollution; (2) Cities with $PM_{2.5}$-O_3 compound pollution have exposure risk levels dominated by ST+ST (Stabilization) and ST+HR (High Risk). Exposure risk levels of compound pollution in developing countries are significantly higher than those in developed countries, with unequal exposure characteristics; (3) The selected cities showed significant positive spatial correlations between $PM_{2.5}$ and O_3 concentrations, which were consistent with the spatial distribution of the precursors NOx and VOCs; (4) During the study period, 52.5% of cities worldwide achieved synergistic reductions in annual average $PM_{2.5}$ and O_3 concentrations. The average $PM_{2.5}$ concentration in these cities decreased by 13.97%, while the average O_3 concentration decreased by 19.18%. This new solution offers the opportunity to construct intelligent and healthy cities in the upcoming low-carbon transition.

Keywords: $PM_{2.5}$-O_3 compound pollution; Population exposure risk; Spatial correlation; Synergistic treatment potential

1. Introduction

Elevated concentrations of fine particulate matter ($PM_{2.5}$) and surface ozone (O_3) are harmful to human health [1,2], ecosystems [3], and crop yields [4,5], and are a major contributor to climate change [6,7]. $PM_{2.5}$ is composed of directly emitted primary $PM_{2.5}$ and secondary $PM_{2.5}$, which is formed from gaseous precursors, including SO_2, Nitrogen Oxides (NOx), Volatile Organic Compounds (VOCs), and NH_3 [8]. O_3 generation, beyond that originating from stratospheric transport, primarily occurs through complex photochemical reactions between NOx and VOCs under sunlight [9]. Recent collaborative efforts by the World Health Organization (WHO) and global governments have led to a notable reduction in $PM_{2.5}$ concentrations worldwide, particularly in certain cities within affluent European and North American nations, where levels have approached or met the WHO's IT-1 target value of 35 μg/m^3 [10]. However, according to data from the 2019 "Global Air Status Report" (https://www.stateofglobalair.org/), 54% of the global population lives in areas above the 35μg/m^3 threshold, resulting in approximately 2.9 million premature deaths from $PM_{2.5}$ exposure. Concurrently, there is growing evidence that global O_3 pollution is becoming more visible, with a wider range of impacts and longer pollution season [11]. According to the Global Burden of Disease (GBD), weighted O_3 concentrations in 11 populous nations range from 45–68 ppb, approaching or exceeding the WHO guideline of 100 μg/m^3. In 2019 alone, O_3 exposure resulted in 365,000 premature deaths worldwide [12]. Amid this context, studies have shown that the health hazards of global air pollution will become more severe in the future, driven by climate change, and that the features of pollution have shifted from single soot-type pollution in the past to compound atmospheric pollution with multiple sources of emissions and multiple pollutants coexisting and interacting with each other [13]. Therefore, clarifying the issue of $PM_{2.5}$ and O_3 compound pollution has become an important atmospheric environmental issue for the next step of improving air quality and realizing environmental sustainability processes globally.

To effectively combat the global pollution caused by $PM_{2.5}$ and O_3 compounds, it is crucial to accurately identify the current challenges, gain knowledge from historical experiences of $PM_{2.5}$ and O_3 pollution management, and ultimately construct a synergistic control framework for $PM_{2.5}$ and O_3 pollution. Recognized as a global menace, scholars have rigorously examined $PM_{2.5}$ and O_3 pollution across diverse spatial scales, delving into their spatiotemporal distribution [14], regional transport mechanisms [15], chemical mechanisms [16,17], drivers [18,19], economic ramifications [20], and health implications [21]. For instance, Zhao et al. [22] examined the worldwide spatial and temporal trends and population exposure risk of $PM_{2.5}$ concentrations from 2000 to 2016, clarifying the relationship between $PM_{2.5}$ concentrations and population exposure risk. From a spatiotemporal lens, Lim et al. [23] identified principal socio-economic elements shaping the spatial alterations in global $PM_{2.5}$ concentrations, subsequently proposing mitigation pathways tailored to nations' economic standings. Approaching from a sustainability perspective, Zhou et al. [24] explored the spatio-temporal trends and population exposure risk of global springtime O_3

concentrations, pinpointing pivotal meteorological determinants influencing different regional O_3 fluctuations and associated human risks. Further, studies by Zhang et al. [25] and Lyu et al. [26] provided comprehensive insights into the health hazards and climate impacts linked to global O_3 pollution.

Concurrently, a plethora of studies have identified a regional synergy in the pollution patterns of $PM_{2.5}$ and O_3. This synergistic feature has been universally observed across cities globally [27]. For instance, Zhao et al. [28] examined the spatiotemporal association of $PM_{2.5}$ and O_3 pollution in 367 key cities in China from 2015 to 2019. Their findings highlighted that those regions with the most severe $PM_{2.5}$ pollution concurrently suffered from intense O_3 pollution. In a similar vein, Sicard et al. [29] scrutinized the interplay between $PM_{2.5}$ and O_3 during air pollution episodes in arid continental climates based on air quality data from 21 ground monitoring stations in the Middle East. They discerned that whenever $PM_{2.5}$ concentrations surged, a concurrent oscillation in O_3 concentrations was evident. Analogous phenomena have been documented in the United States [30] and Europe [31,32] through multi-year air quality monitoring. Moreover, burgeoning evidence posits that $PM_{2.5}$ and O_3 share common precursors, with VOCs and NOx emerging as their most pivotal shared antecedents [33]. On one hand, NOx and VOCs influence $PM_{2.5}$ concentrations by fostering the formation of nitrates and secondary organic aerosols, and simultaneously play a significant role in the chemistry of O_3. On the other hand, the heterogeneous reactions on the surface of particulate matter can directly adsorb O_3 or react with nitrogen oxides (NO_2, NO_3, N_2O_5), thereby affecting O_3 concentration [34]. Specifically, from 2000 to 2019, there was a slight global decrease in $PM_{2.5}$ exposure (on average, -0.2% per year). However, 65% of cities still showed an increasing trend in $PM_{2.5}$ exposure levels. Additionally, the O_3 exposure levels of the global urban population increased (on average, +0.8% per year) due to the reduced titration effect of NO on ozone [35]. Even at night, O_3 levels continued to rise [36]. This shared origin trait of $PM_{2.5}$ and O_3 has been ubiquitously recognized globally. Therefore, coordinated control of $PM_{2.5}$ and O_3 compound pollution from the perspective of synergistic regional emissions and the same sources of $PM_{2.5}$ and O_3 has become the key to managing global compound pollution.

Facing the escalating global challenge of $PM_{2.5}$ and O_3 compound pollution, scholars have embarked on extensive research to elucidate the characteristics of pollution, driving factors, and underlying mechanisms, aiming to devise collaborative mitigation strategies. Such endeavors aspire to offer technical support for the continuous improvement of air quality and public health protection across diverse regions globally. For instance, Wang et al. [37] probed into the causality of $PM_{2.5}$ and O_3 compounded pollution from the perspective of active nitrogen transformation routes in atmospheric nitrogen cycling. Dai et al. [38], leveraging a refined emission inventory of the Yangtze River Delta in China and the WRF-CMAQ model, crafted synergistic control pathways for atmospheric $PM_{2.5}$ and ozone pollution in the region. Ojha et al. [19] reviewed mechanisms and methods for the collaborative control of $PM_{2.5}$ and O_3, positioning it within the context of global warming. Meanwhile, Faridi et al. [39] furnished a comprehensive assessment of long-term trends and health implications of $PM_{2.5}$ and O_3 pollution in Tehran, grounded on real-time hourly concentration datasets from 21 air quality monitoring stations spanning 2006–2015. Such studies grant a pivotal theoretical foundation and empirical insight into the driving forces behind air pollution in various global regions. Nonetheless, there remain gaps in this arena. Historically, many studies gravitated towards analyzing a particular air pollutant, with scant research addressing the spatiotemporal correlation features of compounded pollutants, let alone delving into their intricate interrelations. Further, due to a dearth of pollutant concentration data, assessing the spatiotemporal evolution of pollutants on a global scale remains a challenge. Most critically, there's a conspicuous absence of research offering a holistic understanding of $PM_{2.5}$ and O_3 compounded pollution traits from a global viewpoint, especially within a sustainable development lens that evaluates exposure risks to populations. Concurrently, no framework has been discerned thus far that addresses the collaborative governance of global $PM_{2.5}$ and O_3 compounded pollution.

To address the identified knowledge gaps, this study utilizes $PM_{2.5}$ and O_3 concentration monitoring data from 120 cities globally spanning from 2019 to 2022. Leveraging methodologies such as spatial statistical analysis, time series analysis, exposure risk assessment, and spatial correlation analysis, this research represents the first comprehensive global-scale investigation into the spatiotemporal patterns, evolutionary characteristics, exposure risks, and spatial associations with precursor substances of combined $PM_{2.5}$ and O_3 pollution. This work deepens our understanding of the concurrent management of $PM_{2.5}$ and O_3 on a global scale, proposing an integrated framework for their co-management. The findings stand to foster collaboration between the air quality and climate communities, offering policymakers crucial insights to jointly address these persistently intertwined threats.

2. Materials and methods

2.1. Study area

In this study, we focus on 120 major cities worldwide. These cities are primarily located in Asia (57), Europe (28), North America (22), South America (8), Oceania (3), and Africa (2). The primary reasons for selecting these cities are as follows: Firstly, the chosen cities have high population densities, high anthropogenic emissions, high energy consumption, and elevated levels of air pollution [40–43]. Secondly, data from these cities possess a complete time series, allowing for quantitative analyses over various temporal scales. Lastly, these cities have diverse geographical and climatic conditions. For instance, Beijing has a temperate monsoon climate, while Delhi has a semi-arid climate. These varying geographical and climatic conditions are crucial in enhancing our comprehension of the spatial heterogeneity of $PM_{2.5}$ and O_3 compound pollution. Given these facts, the chosen cities offer a suitable variety of diverse regions for our investigation. Moreover, to delve deeper into the compound pollution status of $PM_{2.5}$ and O_3 at the urban scale, we selected 10 cities out of the 120, namely Beijing (China), Tokyo (Japan), Seoul (South Korea), Delhi (India), Sydney (Australia), London (UK), Rome (Italy), Berlin (Germany), Los Angeles (US), and Mexico City (Mexico) for in-depth analysis. The spatial distribution of the 120 cities and the 10 focus cities is illustrated in Fig. 1.

Fig. 1. Spatial distribution of the study areas. The red dots represent the selected 120 cities, while the green triangles indicate the 10 focal cities (a). The pie chart displays the number of countries from each continent (b), and the bar chart shows the number of cities included from each continent (c).

2.2. Data sources and preprocessing

The daily records of $PM_{2.5}$ and O_3 concentrations across the 120 chosen cities were sourced from the World Air Quality Index (WAQI) portal (https://www.aqicn.org/). To analyze the co-sourced features of $PM_{2.5}$ and O_3 and their effect on the exposure risk of the population, we collected precursor emission inventories (VOCs, NOx) and population inventories from the European

Commission (https://commission.europa.eu/) and The World Bank (https://www.worldbank.org/), respectively. Prior to conducting any analysis, based on the study by He et al. [27], we implemented data quality control measures on the daily $PM_{2.5}$ and O_3 concentrations obtained from 120 cities globally. We discarded anomalous data that did not meet the statistical criteria, such as daily $PM_{2.5}$ and O_3 concentrations that exceeded 999 μg/m^3. In this study, the valid counting days for monthly and annual average concentrations of $PM_{2.5}$ and O_3 in cities are no less than 27 days and 360 days, respectively. Concurrently, this study evaluated the risk of exposure to $PM_{2.5}$ and O_3 pollution with reference to the new Air Quality Guidelines (AQG) issued by the World Health Organization in 2021 [44]. In the specific calculations, we utilized the rolling average of the maximum 8-hour concentrations as the daily average concentration for O_3.

2.3. Definition of $PM_{2.5}$ and O_3 compound pollution

Drawing from past epidemiological studies on the population exposure to $PM_{2.5}$ and O_3 [45,46] and the new AQG standards, we have chosen the daily average concentrations of $PM_{2.5}$ and O_3 to be 35 μg/m^3 and 100 μg/m^3, respectively, as the thresholds for categorizing the dominant pollution types of $PM_{2.5}$ and O_3. Based on this scheme, we classify the dominant pollution types of $PM_{2.5}$ and O_3 into the following four categories: Compound Pollution of $PM_{2.5}$ and O_3 (P-O), $PM_{2.5}$ Dominant Pollution, O_3 Dominant Pollution, and Clean. The detailed categorization criteria are illustrated in Table 1.

Table 1 Compound Pollution Classification Standards

$PM_{2.5}$ (μg/m^3)	**O_3 (μg/m^3)**	**Pollution dominant type**
$\rho(PM_{2.5}) > 35$	$\rho(O_3) > 100$	P-O
$\rho(PM_{2.5}) > 35$	$\rho(O_3) < 100$	$PM_{2.5}$ dominated pollution
$\rho(PM_{2.5}) < 35$	$\rho(O_3) > 100$	O_3 dominated pollution
$\rho(PM_{2.5}) < 35$	$\rho(O_3) < 100$	Clean

2.4. Exposure risk assessment of compound pollution

This study discusses the risk of population exposure to long-term ambient $PM_{2.5}$ and O_3 based on the method by Lim et al. [23]. Initially, we employed the Mann-Kendall method [47,48] to analyze the changing trends of $PM_{2.5}$ and O_3 concentrations over the research period. The calculations for the Mann-Kendall method are as given in Equations 1–4:

$$S = \sum_{i=1}^{n-1} \sum_{j=i+1}^{n} sgn(x_j - x_i) \quad (1)$$

Where: n represents the total number of data points; X_i and X_j are data values in time series i and j. X_j is used as a reference point to compare with the remaining data points X_i. The $sgn(x_j\text{-}x_i)$ is the sign function, with the specific formula as follows:

$$sgn(x_j - x_i) = \begin{cases} +1, & x_j - x_i > 0 \\ 0, & x_j - x_i = 0 \\ -1, & x_j - x_i < 0 \end{cases} \quad (2)$$

Additionally, the formula for calculating the variance is:

$$Var(S) = \frac{1}{18}\left[n(n-1)(2n+5) - \sum_{k=1}^{p} q_k(q_k - 1)(2q_k + 5)\right] \quad (3)$$

In the formula: n represents the total number of data points; p denotes the number of tied groups; q_k indicates the number of data points contained in the k-th tied group. When dealing with large samples ($n > 10$), the standardized test statistic Z is used for calculations:

$$Z = \begin{cases} \frac{S-1}{\sqrt{Var(S)}}, & S > 0 \\ 0, & S = 0 \\ \frac{S+1}{\sqrt{Var(S)}}, & S < 0 \end{cases} \quad (4)$$

By evaluating the Z value, a statistically significant curve trend can be obtained. A positive Z indicates an increasing trend, while a negative Z indicates a decreasing trend. In a two-tailed trend test, for a given confidence level (significance level) α, if $|Z| \geq Z_{1-\alpha/2}$, then the null hypothesis H_0 is rejected. This means that, at the confidence level α, the time series data exhibits a significant increasing or decreasing trend. $|Z|$ values greater than or equal to 1.645, 1.96, and 2.576 represent passing the significance test at confidence levels of 90%, 95%, and 99%, respectively.

Subsequently, combining the high or low levels and change trends of $PM_{2.5}$ or O_3 concentrations, we classified the exposure risk level of the population in different cities under the $PM_{2.5}$ and O_3 environments into six types: High Risk (HR), Stabilization (ST), Risk (R), Deep Stabilization (DST), Safety (S), and High Safety (HS). Among them, HR and ST both indicate extremely high pollutant concentrations, but HR denotes an increasing trend in pollutant concentration, while ST signifies a decreasing trend. R and DST mean high pollutant concentrations with respective increasing and decreasing trends. S and HS indicate low pollutant concentrations, with respective increasing and decreasing trends. Here, based on the epidemiological methods in Strak et al. [49], Guan et al. [45], and Guerreiro et al. [46], we define extremely high pollutant concentration criteria as $\rho(PM_{2.5}) > 35\ \mu g/m^3$ or $\rho(O_3) > 120\ \mu g/m^3$; High pollutant concentration criteria as $25\ \mu g/m^3 < \rho(PM_{2.5}) < 35\ \mu g/m^3$ or $100\ \mu g/m^3 < \rho(O_3) < 120\ \mu g/m^3$; Low pollutant concentration criteria as $\rho(PM_{2.5}) < 25\ \mu g/m^3$ or $\rho(O_3) < 100\ \mu g/m^3$.

2.5. Spatial correlation analysis

In this study, Bivariate Moran's I (Bi-Moran's I), spatial statistical analysis, and spatial correlation analysis models were employed to investigate the spatial agglomeration characteristics, spatial correlations, and spatial associations with the main precursors (NOx and VOCs) of $PM_{2.5}$ and O_3 concentrations in the 120 global cities during the study period. The calculation for the Bi-Moran's I is as per formula 5:

$$I_i^B = cx_i \sum_j w_{ij} y_j \quad (5)$$

In the formula, I_i^B represents the bivariate local Moran's index for region i; w_{ij} is an element of the spatial weight matrix; and c is a constant proportionality factor. This index is used to quantitatively describe the degree of association between variable x in region i and variable y in neighboring region j. Furthermore, the detailed calculation process of the spatial correlation analysis model can be found in the research by Lu et al. [50]. The spatial analyses and implementation involved in this study are primarily conducted using the GeoDa1.20 (http://geodacenter.github.io/), ArcGIS10.7 (https://www.esri.com/), and GWmodelS1.0.3 (https://github.com/GWmodel-Lab/GWmodelS/) software.

2.6. Analysis of synergistic changes in compound pollution

In this study, we measure the level of synergistic changes in $PM_{2.5}$ and O_3 concentrations based on the relative rate of change (*ROC*) of $PM_{2.5}$ and O_3 concentrations in 2019 and 2022, calculated as in Equation 6:

$$If = \begin{cases} ROC_{i,PM_{2.5}} \geq 1 \text{ and } ROC_{i,O_3} \geq 1, & Synergistic\ Increase \\ ROC_{i,PM_{2.5}} < 1 \text{ and } ROC_{i,O_3} < 1, & Synergistic\ Decrease \\ ROC_{i,PM_{2.5}} \geq 1 \text{ and } ROC_{i,O_3} < 1, & PM_{2.5}\ Increase\ and\ O_3\ Decrease \\ ROC_{i,PM_{2.5}} < 1 \text{ and } ROC_{i,O_3} \geq 1, & PM_{2.5}\ Decrease\ and\ O_3\ Increase \end{cases} \tag{6}$$

The *ROCi* in equation is calculated as follows:

$$ROC_i = \frac{C_{i,2022}}{C_{i,2019}} \tag{7}$$

Where *ROC* represents the relative change of $PM_{2.5}$ and O_3 in city *i*. $C_{i,2022}$ and $C_{i,2019}$ represent the concentrations of $PM_{2.5}$ and O_3 in city *i* in 2022 and 2019, respectively.

3. Results

3.1. Temporal and spatial distribution of global $PM_{2.5}$ and O_3 concentrations

Fig. 2a–b depicts the spatial distribution and seasonal variations of the annual average $PM_{2.5}$ concentrations in 120 global cities from 2019 to 2022. The annual average $PM_{2.5}$ concentrations for these cities from 2019 to 2022 were 61.86 μg/m^3, 56.92 μg/m^3, 57.36 μg/m^3, and 55.48 μg/m^3, respectively, indicating a fluctuating downward trend. Among the selected cities, less than 1% were found to have low $PM_{2.5}$ exposures (4-year average $PM_{2.5}$ concentrations ≤ 25 μg/m^3). These cities are primarily situated in Canada, Australia, and several countries in the European Union, such as Vancouver (18.46 μg/m^3), Wollongong (22.17 μg/m^3), and Edinburgh (20.56 μg/m^3). In contrast, high $PM_{2.5}$ concentrations were found in 30% of the cities, where the average concentration of $PM_{2.5}$ over four years exceeded 70 μg/m^3. These cities are mainly found in eastern China, northern and southwestern India, and also include Santiago (Chile, 75.37 μg/m^3) and Johannesburg (South Africa, 75.77 μg/m^3). Notably, northern Indian cities such as Lucknow (146.5 μg/m^3) and Delhi (161.9 μg/m^3) registered 4-year average $PM_{2.5}$ concentrations exceeding 140 μg/m^3. Meanwhile, over 40% of cities had exposures to 4-year average $PM_{2.5}$ concentrations ranging from 35 to 70 μg/m^3, predominantly located in countries such as South Korea, Japan, France, the UK, and Germany. It was observed that the global $PM_{2.5}$ concentrations were at their zenith during the winter and at a nadir during the summer. Compared to summer, the number of cities exposed to lower $PM_{2.5}$ environments in winter decreased by 40%, while those exposed to higher $PM_{2.5}$ levels more than doubled. Such shifts in exposure risk show spatial congruity, particularly in cities in India and China, where regions with milder $PM_{2.5}$ concentrations in summer transition to regions with higher concentrations in winter.

Fig. 2. The spatial distribution of annual average $PM_{2.5}$ and O_3 concentrations in 120 cities globally from 2019 to 2022 (a and c), and the spatiotemporal distribution of $PM_{2.5}$ and O_3 concentrations on a seasonal basis (b and d). The bar chart indicates the number of cities exposed to various $PM_{2.5}$ and O_3 concentration levels.

In the 120 global cities examined, the annual average O_3 concentrations displayed a decline similar to the trends observed for $PM_{2.5}$ concentrations. The O_3 concentrations were noted to decrease from 120.51 μg/m^3 in 2019 to 116.16 μg/m^3 in 2021, further diminishing to 114.57 μg/m^3 in 2022. During the study period, it was found that 50.8% of the cities under consideration exhibited a 4-year average O_3 concentration below 100 μg/m^3. These cities are predominantly located in regions such as the United States (67.6 μg/m^3), Canada (59.4 μg/m^3), Australia (63.6 μg/m^3), and the European Union (71.6 μg/m^3). On the other hand, a smaller portion, around 13.3%, registered a 4-year average O_3 concentration less than 60 μg/m^3. In stark contrast, nearly half of the cities globally presented a 4-year average O_3 concentration surpassing 100 μg/m^3 over the research span. Such cities were chiefly located in India (231.8 μg/m^3), China (169.5 μg/m^3), Japan (121.5 μg/m^3), and South Korea (136.2 μg/m^3). Notably, northern Indian cities like Chennai (217.3 μg/m^3) and Kolkata (265 μg/m^3), as well as Chengdu (173 μg/m^3) in central China, recorded O_3 concentrations far exceeding the O_3 threshold set by the WHO's AQG in 2021. In terms of the seasonal trends, globally, the highest proportion of cities exposed to high O_3 concentrations (> 100 μg/m^3) occurred in summer, representing 19.2% of the selected cities, followed by spring (14.2%), autumn (12.5%), and winter (8.3%). Cities persistently exposed to heightened O_3 environments exhibited distinct spatial clustering, primarily in central China and northeastern India.

In the key cities of focus (Fig. S1.), Delhi registered the pinnacle 4-year average $PM_{2.5}$ concentration at 161.89 ± 60.56 μg/m^3, while Sydney recorded the nadir at 25.03 ± 7.64 μg/m^3. In terms of seasonal variations, $PM_{2.5}$ concentrations in cities such as Berlin, London, Tokyo, Seoul, and Beijing predominantly exhibited a winter > spring > autumn > summer sequence. In contrast, other cities displayed varied seasonal changes: cities like Rome and Sydney peaked in the spring and bottomed out in the summer, while Los Angeles witnessed its minimum concentrations in spring. The highest and lowest O_3 concentrations were identified in Delhi and Rome, respectively, with values of 140.2 ± 37.89 μg/m^3 and 25.34 ± 5.74 μg/m^3. Following closely are Mexico City, Seoul, and Beijing, all of which have O_3 concentrations surpassing 60 μg/m^3. In contrast, other cities exhibit O_3 levels ranging between 30–50 μg/m^3. Additionally, it was observed that the peak O_3 concentrations for these focal cities occurred in summer, while the lowest levels were typically registered in winter (except for Delhi, where the minimum levels were observed in autumn), aligning with the global seasonal variations in O_3 concentrations.

3.2. Global characteristics of $PM_{2.5}$ and O_3 compound pollution

While the $PM_{2.5}$ concentrations in most global cities have yet to reach the thresholds set by AQG, urban O_3 pollution is becoming increasingly severe. There's a noticeable trend of compound pollution involving both $PM_{2.5}$ and O_3 in various global regions. This subsection, based on the methodology provided in Section 2.3, offers a comprehensive analysis of the spatiotemporal variations in $PM_{2.5}$ and O_3 compound pollution across 120 global cities during the research period (Fig. 3). Spatial statistics reveal that only 25.8% of the studied cities enjoy a relatively unpolluted environment (Clean). A significant proportion of these cities reside in the United States, representing approximately 82% of all U.S. cities, with several others in Northern Europe. Conversely, almost half (47.5%) of the global cities evaluated were subjected to $PM_{2.5}$-O_3 compound pollution during the study timeframe. This form of pollution predominantly affected cities in countries such as Chile (4), China (22), South Korea (10), Japan (7), and India (9). Additionally, 25% of cities are exposed to a $PM_{2.5}$ dominant polluted environment, predominantly found in Europe, accounting for roughly 67.9% of European cities (Fig. 3a). From a seasonal perspective, spring, summer, and autumn witness the peak periods for global $PM_{2.5}$-O_3 compound pollution. During these three seasons, an average of over 40% of cities experience $PM_{2.5}$-O_3 compound pollution. Notably, during the summer, almost 50% of the selected cities are exposed to $PM_{2.5}$-O_3 compound pollution. These cities are primarily clustered in South Korea, Eastern and Southern China, and Northern India (Fig. 3b–d). In stark contrast, less than 25% of cities worldwide are exposed to $PM_{2.5}$-O_3 compound pollution in winter, such as Delhi and Mumbai in India, and Shijiazhuang and Chengdu in China. Conversely, during winter, 53.3% of global cities face $PM_{2.5}$ dominant pollution. These cities were dispersed across various continents, with European nations and Northern China marking significant regions for winter $PM_{2.5}$ dominant pollution, for instance, cities like Rome (Italy), Paris (France), and

Hamburg (Germany).

Fig. 3. The spatial distribution (a) and seasonal variation (b) of $PM_{2.5}$-O_3 compound pollution conditions in 120 cities worldwide from 2019 to 2022.

As global air pollution concerns intensify, countries worldwide have issued stringent air pollution control strategies based on their specific conditions, leading to a shift in the dominant forms of air pollution. For the first time, Fig. S2 reveals the spatial characteristics of changes in dominant air pollution types across 120 global cities from 2019 to 2022. Overall, there was a positive shift towards cleaner urban environments: cities classified under the "Clean" category rose from 24 in 2019 to 26 in 2021 and further rose to 31 in 2022. Meanwhile, cities dominated by $PM_{2.5}$ pollution increased slightly from 37 in 2019 to 38 in 2021 but then saw a reduction to 33 by 2022. Furthermore, cities under the bracket of O_3 dominant pollution never exceeded 5% of the analyzed cities throughout the study period. Spatially, our analysis found that 24 cities, such as Berlin and London in Europe, consistently showed $PM_{2.5}$ as the dominant pollutant during the entire study timeframe. In stark contrast, 46 cities persistently witnessed $PM_{2.5}$-O_3 compound pollution. Key cities in this category include Shijiazhuang and Shenyang in China, as well as Delhi and Mumbai in India. Seven cities, primarily situated in parts of India and Europe, transitioned from being $PM_{2.5}$-dominant to experiencing $PM_{2.5}$-O_3 compound pollution. Meanwhile, 11 cities, predominantly located in Japan, some European regions, and Chile (including Yokohama, Lyon, and Rancagua), shifted from the $PM_{2.5}$-O_3 compound pollution to either $PM_{2.5}$ dominant pollution or O_3 dominant pollution. Furthermore, eight cities, dispersed across regions like the US, Australia, and Germany (for example, Chicago, Sydney, and Wiesbaden), transitioned from either O_3 or $PM_{2.5}$ dominant pollution to a "Clean" classification within the research period.

3.3. Exposure risk assessment of compound pollution

The intensification of $PM_{2.5}$ and O_3 pollutants in the atmosphere presents diverse environmental exposure risks in cities globally. Fig. 4 illustrates the spatial distribution of air pollution exposure risks in 120 global cities during the study period. Our analysis identifies the primary types of compound pollution exposure risks in global cities as ST+ST, ST+HS, DST+HS,

ST+DST, ST+HR, ST+DST, ST+HR, HS+HS, ST+HS, and DST+HS. Notably, ST+ST and ST+HS emerge as the most critical exposure risk types related to $PM_{2.5}$-O_3 compound pollution. Among the selected cities, 29 exhibit the ST+ST exposure risk type, predominantly located in China, Korea, Japan, India, and Chile. Characterized by $PM_{2.5}$ and O_3 concentrations exceeding 35 μg/m^3 and 100 μg/m^3 respectively, these cities, though witnessing a declining trend, will subject their populations to significant compound pollution risks in the future. In contrast, 23 cities worldwide manifest the ST+HS compound pollution exposure risk type, mainly situated in Thailand, the UK, France, and Germany. Such cities, while presenting $PM_{2.5}$ concentrations above 35 μg/m^3 and O_3 concentrations below 100 μg/m^3, display a substantial decline in pollutant concentrations. Consequently, while they currently experience significant compound pollution risks, the consistent decline in O_3 levels suggests a hopeful trajectory towards reduced risks. Additionally, 12, 10, and 10 cities globally show compound pollution exposure risks of DST+HS, ST+DST, and ST+HR, respectively. This includes Chicago, Boston, and Miami in the US, Shijiazhuang and Qingdao in China, and Delhi and Lucknow in India. In these cities, at least one of the $PM_{2.5}$ or O_3 concentrations falls below the AQG threshold and exhibits a continued declining trend, which results in a gradual reduction in compound pollution risks. From a demographic perspective, in densely populated Asian regions (over 200 million), the compound pollution risks are largely categorized into three types: ST+DST (10), ST+HR (10), and ST+ST (25). In Europe, a cumulative population exceeding 20 million is exposed to environments with compound pollution risk levels of HS+HS (5) and ST+HS (15). In North America, the predominant exposure risk is DST+HS (7).

Fig. 4. (a) Exposure risk assessment of compound pollution across 120 cities from 2019 to 2022; the line chart indicates the population count; the heatmap shows the number of city sites under different compound pollution exposure risks. (b–c) $PM_{2.5}$ and O_3 pollution exposure risk assessment for 120 cities from 2019 to 2022. (d) Exposure risk assessment for select cities from 2019 to 2022; blue borders represent cities in developed countries, and green borders indicate cities in developing countries. Smaller square or oval borders suggest a city population of less than 1 million (10^6), while larger ones indicate the opposite.

The analysis of the individual trends in $PM_{2.5}$ and O_3 concentrations shows that approximately

63.3% (or 76) of cities worldwide are exposed to an environment with a $PM_{2.5}$ risk type of ST. These cities are primarily located in Germany, France, China, India, Korea, Japan, Thailand, and Chile, with examples including Tokyo, Busan, Chongqing, Lucknow, Rome, Paris, and Santiago. Furthermore, cities with a $PM_{2.5}$ exposure risk type of DST account for about 14.2% globally. They are predominantly found in the eastern and southern parts of the USA, as well as in southeastern Canada, like Toronto and Chicago. Moreover, it was noted that approximately 16.7% of the cities globally present $PM_{2.5}$ exposure risks classified as R and HR. These cities, primarily located in the western USA—including Phoenix and Philadelphia—display $PM_{2.5}$ concentrations oscillating between 25–35 μg/m^3 and exceeding 35 μg/m^3, respectively, both indicating an increasing pattern. Additionally, a combined 5.8% of the cities, exemplified by Vancouver, exhibited $PM_{2.5}$ exposure risks defined as HS and S, characterized by concentrations under 25 μg/m^3. It's noteworthy that those within the 'S' classification reveal a rising $PM_{2.5}$ trend (Fig. 4b). Regarding O_3, over 50% of cities worldwide have O_3 exposure risk types of HS and S. These cities are largely spread across the eastern USA and most European regions, such as Berlin, London, and Miami. Additionally, cities with O_3 exposure risk types of ST or HR are primarily located in northern India, eastern China, Korea, and Japan. Among these, cities with an exposure risk type of HR represent 12.5% and are chiefly centered in southeastern China, including cities like Shanghai and Jinan (Fig. 4c). From a combined perspective of population and economic levels, cities exposed to $PM_{2.5}$ (or O_3) concentrations below 35 μg/m^3 (or 120 μg/m^3) are largely found in developed countries. Examples are Chicago (US), San Antonio (US), Helsinki (Finland), and Sydney (Australia). About 125 million people in these areas can enjoy the reduced exposure risks brought by good air quality (low pollutant concentrations). In stark contrast, cities in developing nations like Beijing, Mumbai, and Delhi continue grappling with exacerbated pollutant concentrations. An estimated populace of 218 million endures heightened pollution environments, consequently intensifying their vulnerability to associated exposure risks.

3.4. Spatial association between $PM_{2.5}$-O_3 compound pollution and precursors

The environmental exposure risks caused by $PM_{2.5}$-O_3 compound pollution are increasingly severe. A quantitative elucidation of the spatial correlation between $PM_{2.5}$ and O_3 concentrations, along with their spatial association with precursors, holds paramount importance for devising coordinated emission reduction strategies for $PM_{2.5}$ and O_3 concentrations under forthcoming sustainable development paradigms. In Fig. 5a–b, the scatter plot of $PM_{2.5}$-O_3 bivariate Moran's I and the spatial clustering distribution for 120 global city stations are depicted. It can be observed that the bivariate Moran's I for $PM_{2.5}$ and O_3 is 0.435 (Moran's I > 0 indicates clustering), and it has passed the significance test ($P < 0.05$). Such results underscore a significant positive spatial correlation between $PM_{2.5}$ and O_3 concentrations. Specifically, 43 cities worldwide have their bivariate Moran's I for $PM_{2.5}$ and O_3 concentrations in the first quadrant, indicating a High-High spatial clustering pattern. Predominantly, these cities are located in regions such as China, India, Korea, and Thailand, marked by high levels of both $PM_{2.5}$ and O_3 concentrations. Meanwhile, bivariate Moran's I for $PM_{2.5}$ and O_3 concentrations in 48 cities, mainly in the USA, Canada, the UK, and France, were observed in the third quadrant, indicating a Low-Low spatial clustering pattern with low $PM_{2.5}$ and O_3 concentrations. In addition, certain cities in Japan and Mexico were ascertained to manifest either a Low-High or High-Low spatial clustering paradigm.

To further study the spatial association features between $PM_{2.5}$ and O_3 concentrations, we employed spatial correlation analysis methods to quantitatively reveal the correlation between $PM_{2.5}$ and O_3 concentrations. The results indicate that the correlation coefficient (Correlation) of $PM_{2.5}$-O_3 for the selected cities during the study period is all greater than zero, indicative of a positive correlation between $PM_{2.5}$ and O_3 concentrations. Specifically, in 58 cities located in eastern China, Japan, Korea, the western USA, and central Chile, the correlation coefficient of $PM_{2.5}$ and O_3 concentrations exceeded 0.6. In 41 cities in India, the UK, and the eastern USA, this coefficient ranged between 0.4 and 0.6, such as in Delhi (0.584), Miami (0.443), and London (0.441). Additionally, fewer than 25 cities, predominantly in central and southern Europe, exhibited a Correlation below 0.4, with cities like Madrid and Zürich registering 0.3 and 0.202, respectively. Upon conducting multivariate regression analyses on $PM_{2.5}$ and the correlation coefficient ($R^2 = 0.13128$), it was discerned that as $PM_{2.5}$ concentration remained below 110 μg/m^3 (STD: 1.717), the Correlation increased concomitant with the elevation of $PM_{2.5}$ concentration. However, upon reaching a peak value of 0.623, the Correlation began to wane with increasing $PM_{2.5}$ concentrations. These observations suggest that over 60% of cities worldwide exhibit a marked synergistic fluctuation between $PM_{2.5}$ and O_3 concentrations, underscoring the potential for coordinated management approaches in subsequent years. Significantly, through the analysis of the potential spatial associations between $PM_{2.5}$ and O_3 concentrations and their predominant precursors (NOx and VOCs), it was ascertained that regions in China and India, characterized by elevated $PM_{2.5}$ and O_3 concentrations, also reported the highest emissions of NOx and VOCs, each exceeding an annual emission threshold of 1 million tons. Trailing them was the west coast of the USA, with annual emissions of NOx and VOCs surpassing 500,000 tons. Such findings underscore the pivotal role that the cumulative emission effects of NOx and VOCs assume in shaping regional atmospheric pollution.

Fig. 5. Distribution of $PM_{2.5}$-O_3 Bi-Moran's I and spatial distribution characteristics for 120 city sites from 2019 to 2022 (a–b); Global spatial distribution of NOx and VOCs (c–d); Spatial distribution characteristics and trend features of the spatial correlation coefficient of $PM_{2.5}$-O_3 for 120 city sites from 2019 to 2022 (e–f).

3.5. Potential for global coordinated management of $PM_{2.5}$-O_3 compound pollution

Based on the preceding sections, it can be conclusively deduced that $PM_{2.5}$-O_3 compound pollution manifests characteristics of overlapping pollution types, intertwined processes, and interactions across multiple scales. These distinct features serve as a robust scientific underpinning for the evaluation of potential coordinated management of $PM_{2.5}$-O_3 compound pollution, as depicted in Fig.6a. In this segment, the potential was analyzed by examining the ratio of annual average concentration changes of $PM_{2.5}$ and O_3 between 2019 and 2022 across 120 global cities (Fig.6b–c). Statistical results indicate that between 2019 and 2022, 63 cities achieved a coordinated decline in the annual average concentrations of $PM_{2.5}$ and O_3, representing 52.5% of the total cities studied. These cities registered an average decrease of 13.97% in $PM_{2.5}$ and 19.18% in O_3 concentrations. Geographically, a majority of these cities are situated in China (16), South Korea (8), and Japan (7). In contrast, 14 cities, representing 11.67% of the total, experienced a concurrent augmentation in the annual average concentrations of $PM_{2.5}$ and O_3 during the assessment period. Their average concentrations surged by 6.17% and 23.99%, respectively. Predominantly, these cities are located in the USA (6) and India (2). Furthermore, a seesaw effect—characterized by a decrease in $PM_{2.5}$ concentration concurrent with an increase in O_3 concentration, or vice versa—was observed in the annual average concentrations of $PM_{2.5}$ and O_3 in 43 cities throughout the study's duration. These cities spanned diverse global locations, with the Asian region (20) exhibiting the most marked seesaw effect.

Fig. 6. Mechanism features of $PM_{2.5}$-O_3 compound pollution (a), quadrant distribution of regional synergistic management potential (b), and spatial distribution (c). Specifically, Fig.6b categorizes the variations in $PM_{2.5}$ and O_3 concentrations into the following four types based on their ratio: Synchronized increase of $PM_{2.5}$ and O_3 concentrations (First quadrant, both $PM_{2.5}$ and O_3 concentration ratios > 1); Increase in $PM_{2.5}$ concentration with a decrease in O_3 concentration (Second quadrant, $PM_{2.5}$ concentration ratio > 1 and O_3 concentration ratio < 1); Synchronized decrease of $PM_{2.5}$ and O_3 concentrations (Third quadrant, both $PM_{2.5}$ and O_3 concentration ratios < 1); Decrease in $PM_{2.5}$ concentration with an increase in O_3 concentration (Fourth quadrant, $PM_{2.5}$ concentration ratio < 1 and O_3 concentration ratio > 1). The bar chart in Fig.6c indicates the number of cities for each synergistic change type.

4. Discussion

4.1. $PM_{2.5}$ and O_3 compound pollution and synergistic control of spatial heterogeneity

The cities with frequent $PM_{2.5}$ and O_3 compound pollution are mainly in the Asian region, especially in China and India, where the number of compound pollution episodes is higher than in other regions, and the exposure risk of $PM_{2.5}$ and O_3 compound pollution was at the ST+ST level during the study period. One of the most important reasons for this is the high-speed economic development that has led to significant anthropogenic emissions, particularly of VOCs and NOx, which are precursors that promote O_3 production [51–53]. For instance, Beijing and the Pearl River Delta (PRD) in China had effectively controlled particulate matter pollution, represented by $PM_{2.5}$, after the implementation of the Action Plan for the Prevention and Control of Air Pollution. However, compound pollution with high concentrations of $PM_{2.5}$ and O_3 has become the main problem nowadays. There are multiple reasons contributing to this change, but the fundamental reason is the higher emission intensity in these regions, while the meteorological conditions have been more favorable for O_3 generation in recent years [55–59]. Furthermore, at the O_3 chemistry level, this phenomenon occurs because the effects of precursors NOx and VOCs are not linear, and O_3 concentrations may rebound as NOx emissions are reduced [60–62]. Similarly, the main reason for the sharp increase in O_3 concentrations in India in recent years is closely related to the emission of O_3 precursors. According to Chen et al. [63], reducing NOx emissions by 50% in India in 2018 resulted in a 10% to 50% increase in O_3. Conversely, a 50% reduction in VOC emissions can lead to a 60% reduction in O_3. In 2019, India's annual average $PM_{2.5}$ concentration was 91.7 μg/m^3, which is still higher than the WHO IT-1 (35 μg/m^3) [64]. This means that while India has not yet met the $PM_{2.5}$ standard, O_3 pollution has increased, resulting in more compound pollution events.

Compared to Asian cities, European and North American cities have relatively low levels of $PM_{2.5}$ and O_3 compound pollution. This pollution is mainly dominated by either $PM_{2.5}$ or O_3, and most of the population exposure risk status is DST+HS and ST+HS. The industrial structure of most cities in Europe and North America is dominated by tertiary and emerging industries, which are most notably characterized by low emissions and high returns. Compared to most Asian cities that are still reliant on secondary industries, Europe and North America have lower levels of industrial emissions, which means that $PM_{2.5}$ concentrations are also significantly lower than in Asian cities [8,65–67]. Some North American cities have $PM_{2.5}$ concentrations that reach the AQG levels set by the WHO. Unfortunately, increased emissions of ozone precursors and unfavorable meteorological factors have led to O_3 pollution becoming a new challenge to atmospheric pollution in some North American and European cities [68,69]. Equally important, air pollution in the eastern United States and southern Europe has been worsened by wildfires and cross-border pollutant transport, which has serious implications for the health of regional populations [70,71].

Analysis of the characterization of synergistic emissions of $PM_{2.5}$ and O_3 reveals that there is a significant positive spatial correlation between global $PM_{2.5}$ and O_3 concentrations. This relationship is mainly determined by the homology of $PM_{2.5}$ and O_3 concentrations. Previous studies have shown that $PM_{2.5}$ precursors include SO_2, NOx, NH_3, VOCs, and primary $PM_{2.5}$. Among these, NOx and VOCs are the most significant precursors in O_3 chemistry [72,73]. At the same time, we find significant spatial consistency between the spatial and temporal patterns of global NOx and VOC emissions and the associated strengths of $PM_{2.5}$ and O_3 concentrations. In other words, regions with stronger spatial correlation between $PM_{2.5}$ and O_3 concentrations have higher emissions of NOx and VOCs, further suggesting that synergistic emission reduction of NOx and VOCs is key to achieving synergistic control of $PM_{2.5}$ and O_3, for example, pollutants such as VOCs, NOx, etc. can be reacted into other compounds by electrocatalysis and thermal catalysis [74,75]. From the characteristics of synergistic changes in $PM_{2.5}$ and O_3 concentrations, 52.5% of the selected cities showed synergistic decreases. These cities are mainly located in East and South Asia. Appropriate adjustment of industrial layout in the future will greatly reduce the trend of $PM_{2.5}$ and O_3 compound pollution in these cities and realize sustainable development.

4.2. $PM_{2.5}$-O_3 correlation analysis of key cities

Through correlation analysis, we found high correlation areas and seasonal characteristics of $PM_{2.5}$ and O_3 concentrations. In Asian cities, particularly in East and South Asia, the interactions are greater because the static weather conditions in winter caused by Siberian high pressure often reduce vertical mixing in the atmosphere, leading to a build-up of pollutants close to the ground [76,77]. In addition, high summer temperatures and intense solar radiation provide favorable conditions for O_3 formation in the tropical and subtropical regions of Asia. However, in monsoon climates, increased rainfall may wash out atmospheric pollutants, including precursors of O_3. Previous studies have identified wind speed and shortwave radiation as the primary factors contributing to the fluctuations in $PM_{2.5}$ concentrations in the Beijing area [78,79]. For O_3, temperature is the most important correlation factor that affects its change [80]. Furthermore, based on research into air pollution mechanisms, it has been discovered that there is a strong positive correlation between $PM_{2.5}$ concentration and extinction coefficient. Additionally, carbon-containing aerosols, which are one of the main components of aerosols, can also absorb light [81,82]. Therefore, areas with high concentrations of $PM_{2.5}$, meaning high levels of atmospheric aerosols, will have a greater impact on local light intensity and, consequently, on the local production of O_3 [9,83]. Previous studies have indicated that $PM_{2.5}$ and O_3 concentrations in Delhi exhibit distinct seasonal trends, with differences between summer and winter. Therefore, it is recommended to analyze them separately on a seasonal basis. During winter, high concentrations of $PM_{2.5}$ have a significant impact on incident solar radiation, which affects O_3 concentrations. In summer, $PM_{2.5}$ is diluted due to ventilation effects, but O_3 concentrations increase due to atmospheric oxidation [84–86]. In contrast, while Tokyo and Seoul have significantly better environmental levels than most Chinese and Indian cities, they still fall short of meeting WHO standards. The chemical industry and combustion source sectors in Japan have a significant impact on local VOC emissions, which indirectly contribute to local $PM_{2.5}$ and O_3 pollution [87]. The establishment of a "Road Transport" department in Seoul has led to an increase in the number of registered vehicles and kilometers driven, resulting in increased local $PM_{2.5}$ and O_3 pollution [88].

Air pollution is generally less problematic in Europe than in Asia due to milder climatic conditions and better atmospheric dispersion. However, seasonal peaks in $PM_{2.5}$ occur during the winter months due to increased heating demand. Moderate high temperatures in Europe promote the formation of O_3. However, extensive environmental policies and emission controls have reduced O_3 precursor emissions, aiding in the regulation of O_3 levels. In general, the more moderate changes in $PM_{2.5}$ and O_3 concentrations in the European region and the observed positive correlation between $PM_{2.5}$ and O_3 concentrations may be due to the decisive role of secondary photochemical processes in the formation of secondary particulate matter, especially in the absence of anthropogenic sources [89]. Previous studies have shown that the most significant sources of O_3 and $PM_{2.5}$ in London, Berlin, and Rome are boundary conditions, transport, biological emissions, and heating systems in winter [90,91]. For London, the most significant non-road transport emissions are likely from shipping activities in the English Channel [92].

In North America, industrial activities and automobile use are significant sources of $PM_{2.5}$, particularly in urban and industrially dense areas. However, environmental regulations and policies, such as the Clean Air Act, help to control $PM_{2.5}$ emissions. In addition, the transportation of pollutants across borders and high local ambient temperatures may exacerbate environmental pollution [93]. Environmental studies have reported that the composition of $PM_{2.5}$ varies in areas of different dimensions due to factors such as geographical and climatic conditions, socio-economic status, and local industrial emissions [94,95]. These differences in $PM_{2.5}$ composition may affect the interaction between $PM_{2.5}$ and O_3 [96]. Although Los Angeles is considered to be one of the most polluted areas in the United States, its pollution levels are still lower than those of many cities in Asia [97]. Stricter emission standards have effectively controlled VOCs and NOx emissions in Los Angeles by reducing motor vehicle emissions, including petrol evaporation [98–100]. Mexico City has successfully reduced primary pollutant emissions over the past few decades. However, it still faces challenges in reducing secondary pollutant emissions, such as $PM_{2.5}$ [101]. Previous studies have shown that the main reason for high local levels of O_3 and $PM_{2.5}$ during the outbreak closure was air quality exchange through valley passages. Domestic heating is a major contributor to local $PM_{2.5}$ pollution, and increased solar radiation and household activities also contribute to O_3 pollution [102].

Previous studies have shown that reducing emissions from wood heaters and power stations in the Sydney area can extend the life expectancy of the local population and have a positive impact on the local economy [103]. Sydney has experienced mild temperatures and meteorological conditions throughout the year. However, due to the intensification of the heat island cycle and the enhancement of urban roughness, there has been a heightened correlation between temperature and wind speed on local O_3 concentrations. Additionally, there has been a high frequency of O_3 and $PM_{2.5}$ pollution extremes that are strongly correlated with the worsening of local hill fire events [104].

4.3. Policy and recommendations

In this study, we reveal the dynamic change characteristics of global $PM_{2.5}$ and O_3 compound pollution, exposure risk level, spatial clustering characteristics, and synergistic change rules, and propose the following policies and recommendations for global $PM_{2.5}$ and O_3 pollution treatment.

(1) As implications for future air pollution mitigation strategies, developed cities are advised to prioritize preventive pollution measures, ensuring the curtailment of high pollution incidents potentially triggered by unfavorable meteorological conditions or human-induced emissions. On the contrary, for cities in developing countries, like Delhi in India and the Beijing-Tianjin-Hebei region in China, it's imperative to draft strict air pollution control policies while placing emphasis on regional economic growth. Simultaneously, there should be proactive promotion of the green transformation of traditional industries, aiming to minimize industrial emissions, residential emissions, and transport-related emissions resulting from the growth of conventional industries.

(2) To meet the stipulated benchmarks for $PM_{2.5}$ and O_3, regions severely affected by compound pollution (such as China and India) should focus on strengthening end-point control measures in the industrial and transportation sectors, emphasize adjusting the industrial structure and substituting sources for processes like petrochemicals, industrial painting, and wood furniture, and optimize the energy structure of motor vehicles.

(3) Broadly speaking, in order to address the inequalities in air pollution exposure and

associated risks, governmental departments across countries should actively explore spatial variations of air pollution exposure inequalities and their potential determinants under the 2030 United Nations Sustainable Development Goals. Economic development, income levels, industrial adjustments, education standards, and racial considerations should be incorporated into regional and national environmental health plans. It is vital to synchronize regional air pollution interventions with enhancements in healthcare. Addressing the challenges of unequal air pollution exposure is integral to forging a sustainable society.

(4) For regions achieving a coordinated decrease in $PM_{2.5}$ and O_3, local governmental departments should further refine the implementation plans for synergistic management of air pollutants and establish robust mechanisms to prevent a resurgence of $PM_{2.5}$-O_3 compound pollution events. For areas witnessing synchronized increases in $PM_{2.5}$ and O_3 concentrations, we recommend initially constructing high temporal and spatial resolution regional emission inventories, understanding the pollution mechanisms and potential sources of $PM_{2.5}$ and O_3 from atmospheric chemistry and regional transmission perspectives, and formulating targeted pollution reduction policies based on these findings.

Overall, such initiatives are crucial for promoting both high-quality ecological protection and high-quality economic development collaboratively.

4.4. Research limitations and prospects

This study has some limitations. It focuses on a short-term period from 2019 to 2022 to analyze the trends of $PM_{2.5}$ and O_3 concentrations. Typically, a 10-year time series is considered sufficient to assess short-term changes in air pollution levels, attributing observed fluctuations predominantly to changes in emissions rather than meteorological variations. The decision to focus on a shorter timeframe in this study is primarily driven by the emergent nature of $PM_{2.5}$-O_3 compound pollution challenges and the urgency in addressing them. However, this approach does bear limitations. The relatively brief period may not fully encapsulate the broader impacts of long-term meteorological patterns and emission change trends on air quality. As such, the findings presented herein should be interpreted with caution, acknowledging the potential for meteorological variations to influence the observed pollution levels over this period. To mitigate these limitations, this study incorporates a review of existing literature and attempts to contextualize the findings within the broader scope of ongoing research in the field of air quality and pollution control. By highlighting these limitations, the study aims to provide a transparent and critical assessment of its findings, contributing to the ongoing discourse on effective strategies for $PM_{2.5}$ and O_3 pollution management and encouraging further research that addresses these emerging challenges with a longer temporal analysis.

Furthermore, we will expand the temporal scope of our analysis by incorporating longer time series data. This will enable us to more accurately identify the underlying trends in $PM_{2.5}$ and O_3 pollution. Future research will seek to disentangle the respective contributions of changes in emissions and meteorological forcing over longer periods, thereby deepening our understanding of the dynamics governing air quality. Exploring the effectiveness of pollution control strategies across different meteorological and geographical contexts is crucial for developing more nuanced and effective approaches to air pollution management.

5. Conclusions

During the study period, globally, 30% and 50% of cities were exposed to high $PM_{2.5}$ (>70 μg/m^3) and O_3 (>100 μg/m^3) concentrations respectively. Elevated concentrations of $PM_{2.5}$ and O_3 were predominantly observed in cities of developing nations, notably China and India. Furthermore, it was noted that over 80% of global cities encountered peak $PM_{2.5}$ values during winter, whereas peak O_3 values were predominantly identified during summer months. Nearly 50% of cities worldwide were affected by $PM_{2.5}$-O_3 compound pollution. Countries like China, South Korea, Japan, and India suffered the most severe impacts from $PM_{2.5}$-O_3 compound pollution. With the exacerbation of O_3 pollution from 2019 to 2022, it was observed that 44.2% of cities globally transitioned from being primarily affected by $PM_{2.5}$ or other contaminants to a predominant influence of $PM_{2.5}$-O_3 compound pollution. Over 40 cities were identified in areas of high exposure risk to this compound pollution, with exposure risk types classified as Stabilization + Stabilization (29), Stabilization + High Risk (10), and High Risk + High Risk (4). From the perspective of regional economic levels, there is an inequality in exposure risk due to $PM_{2.5}$-O_3 compound pollution. Specifically, cities in developing nations were found to be at higher risk compared to their counterparts in developed countries. Between 2019 and 2022, 52.5% of cities worldwide achieved a coordinated decline in the annual average concentrations of $PM_{2.5}$ and O_3. These cities witnessed an average drop of 13.97% for $PM_{2.5}$ and 19.18% for O_3 concentrations. Notably, there was a significant spatial clustering characteristic in the concentrations of $PM_{2.5}$ and O_3 in these cities, accompanied by a positive spatial correlation. Additionally, nearly 12% of cities saw a synchronized increase in the annual average concentrations of $PM_{2.5}$ and O_3.

CRediT authorship contribution statement

C.H.: supervision, conceptualization, writing–original draft, writing–review &editing; J.H.L.: visualization, writing–original draft; Y.Q.Z.: data curation, resources; J.W.Z.: software; L.Z.: methodology; Y.F.W.: Investigation; L.L., S.P.: supervision.

Declaration of competing interests

The authors declare that they have no known competing financial interests or personal relationships that could have appeared to influence the work reported in this paper.

Reference

[1] P. Sicard, O. Lesne, N. Alexandre, A. Mangin, R. Collomp, Air quality trends and potential health effects – Development of an aggregate risk index, Atmospheric Environment. 45(5) (2011) 1145-1153. https://doi.org/10.1016/j.atmosenv.2010.12.052.

[2] Z.L. Fleming, R.M. Doherty, E. von Schneidemesser, C.S. Malley, O.R. Cooper, J.P. Pinto, et al., Tropospheric Ozone Assessment Report: Present-day ozone distribution and trends relevant to human health, Elementa: Science of the Anthropocene. 6 (2018). https://doi.org/10.1525/elementa.273.

[3] N. Unger, Y. Zheng, X. Yue, K.L. Harper, Mitigation of ozone damage to the world's land ecosystems by source sector, Nature Climate Change. 10(2) (2020) 134-137. https://doi.org/10.1038/s41558-019-0678-3.

[4] L. Emberson, Effects of ozone on agriculture, forests and grasslands, Philosophical transactions. Series A, Mathematical, physical, and engineering sciences. 378 (2020) 20190327. https://doi.org/10.1098/rsta.2019.0327.

[5] L. Zhou, X. Chen, X. Tian, The impact of fine particulate matter ($PM_{2.5}$) on China's agricultural production from 2001 to 2010, Journal of Cleaner Production. 178 (2018) 133-141. https://doi.org/10.1016/j.jclepro.2017.12.204.

[6] P.L. Kinney, Interactions of Climate Change, Air Pollution, and Human Health, Current Environmental Health Reports. 5(1) (2018) 179-186. https://doi.org/10.1007/s40572-018-0188-x.

[7] D. Shindell, G. Faluvegi, A. Lacis, J. Hansen, R. Ruedy, E. Aguilar, Role of tropospheric ozone increases in 20th-century climate change, Journal of Geophysical Research: Atmospheres. 111(D8) (2006). https://doi.org/10.1029/2005JD006348.

[8] E.E. McDuffie, R.V. Martin, J.V. Spadaro, R. Burnett, S.J. Smith, P. O'Rourke, et al., Source sector and fuel contributions to ambient $PM_{2.5}$ and attributable mortality across multiple spatial scales, Nature Communications. 12(1) (2021) 3594. https://doi.org/10.1038/s41467-021-23853-y.

[9] R. Atkinson, Atmospheric chemistry of VOCs and NOx, Atmospheric Environment. 34(12) (2000) 2063-2101. https://doi.org/10.1016/S1352-2310(99)00460-4.

[10] C. Li, A. van Donkelaar, M.S. Hammer, E.E. McDuffie, R.T. Burnett, J.V. Spadaro, et al., Reversal of trends in global fine particulate matter air pollution, Nature Communications. 14(1) (2023) 5349. https://doi.org/10.1038/s41467-023-41086-z.

[11] O.R. Cooper, M.G. Schultz, S. Schröder, K.-L. Chang, A. Gaudel, G.C. Benítez, et al., Multi-decadal surface ozone trends at globally distributed remote locations, Elementa: Science of the Anthropocene. 8 (2020) 23. https://doi.org/10.1525/elementa.420.

[12] C.J.L. Murray, A.Y. Aravkin, P. Zheng, C. Abbafati, K.M. Abbas, M. Abbasi-Kangevari, et al. Global burden of 87 risk factors in 204 countries and territories, 1990–2019: a systematic analysis for the Global Burden of Disease Study 2019, The Lancet. 396(10258) (2020) 1223-1249. https://doi.org/10.1016/S0140-6736(20)30752-2.

[13] T. Zhu, Air pollution in China: scientific challenges and policy implications, National Science Review. 4(6) (2018) 800-800. https://doi.org/10.1093/nsr/nwx151.

[14] H. Yue, Q. Huang, C. He, X. Zhang, Z. Fang, Spatiotemporal patterns of global air pollution: A multi-scale landscape analysis based on dust and sea-salt removed $PM_{2.5}$ data, Journal of Cleaner Production. 252 (2020) 119887. https://doi.org/10.1016/j.jclepro.2019.119887.

[15] Y. Bai, T. Zhao, W. Hu, Y. Zhou, J. Xiong, Y. Wang, et al., Meteorological mechanism of regional $PM_{2.5}$ transport building a receptor region for heavy air pollution over Central China, Science of The Total Environment. 808 (2022) 151951. https://doi.org/10.1016/j.scitotenv.2021.151951.

[16] S. Wang, R. Yu, H. Shen, S. Wang, Q. Hu, J. Cui, et al., Chemical characteristics, sources, and formation mechanisms of $PM_{2.5}$ before and during the Spring Festival in a coastal city in Southeast China, Environmental Pollution. 251 (2019) 442-452. https://doi.org/10.1016/j.envpol.2019.04.050.

[17] Y. Zhao, Y. Li, A. Kumar, Q. Ying, F. Vandenberghe, M.J. Kleeman, Separately resolving NOx and VOC contributions to ozone formation, Atmospheric Environment. 285 (2022) 119224. https://doi.org/10.1016/j.atmosenv.2022.119224.

[18] T. Xu, C. Zhang, C. Liu, Q. Hu, Variability of $PM_{2.5}$ and O_3 concentrations and their driving forces over Chinese megacities during 2018-2020, Journal of Environmental Sciences. 124 (2023) 1-10. https://doi.org/10.1016/j.jes.2021.10.014.

[19] N. Ojha, M. Soni, M. Kumar, S.S. Gunthe, Y. Chen, T.U. Ansari, Mechanisms and Pathways for Coordinated Control of Fine Particulate Matter and Ozone, Current Pollution Reports. 8(4) (2022) 594-604. https://doi.org/10.1007/s40726-022-00229-4.

[20] Y. Wang, J. Hu, J. Zhu, J. Li, M. Qin, H. Liao, et al., Health Burden and economic impacts attributed to $PM_{2.5}$ and O_3 in china from 2010 to 2050 under different representative concentration pathway scenarios, Resources, Conservation and Recycling. 173 (2021) 105731. https://doi.org/10.1016/j.resconrec.2021.105731.

[21] U. Im, S.E. Bauer, L.M. Frohn, C. Geels, K. Tsigaridis, J. Brandt, Present-day and future $PM_{2.5}$ and O_3-related global and regional premature mortality in the EVAv6.0 health impact assessment model, Environmental Research. 216 (2023) 114702. https://doi.org/10.1016/j.envres.2022.114702.

[22] C. Zhao, J. Pan, L. Zhang, Spatio-temporal patterns of global population exposure risk of $PM_{2.5}$ from 2000–2016, Sustainability. (2021). https://doi.org/10.3390/su13137427.

[23] C.-H. Lim, J. Ryu, Y. Choi, S.W. Jeon, W.-K. Lee, Understanding global $PM_{2.5}$ concentrations and their drivers in recent decades (1998–2016), Environment International. 144 (2020) 106011. https://doi.org/10.1016/j.envint.2020.106011.

[24] Y. Zhou, W. Duan, Y. Chen, J. Yi, B. Wang, Y. Di, et al., Exposure Risk of Global Surface O_3 During the Boreal Spring Season, Exposure and Health. 14(2) (2022) 431-446. https://doi.org/10.1007/s12403-022-00463-7.

[25] Y. Zhang, J.J. West, L.K. Emmons, J. Flemming, J.E. Jonson, M.T. Lund, et al., Contributions of World Regions to the Global Tropospheric Ozone Burden Change From 1980 to 2010, Geophysical Research Letters. 48(1) (2021) e2020GL089184. https://doi.org/10.1029/2020GL089184.

[26] X. Lyu, K. Li, H. Guo, L. Morawska, B. Zhou, Y. Zeren, et al., A synergistic ozone-climate control to address emerging ozone pollution challenges, One Earth. 6(8) (2023) 964-977. https://doi.org/10.1016/j.oneear.2023.07.004.

[27] C. He, S. Hong, L. Zhang, H. Mu, A. Xin, Y. Zhou, et al., Global, continental, and national variation in $PM_{2.5}$, O_3, and NO2 concentrations during the early 2020 COVID-19 lockdown, Atmospheric Pollution Research. 12(3) (2021) 136-145. https://doi.org/10.1016/j.apr.2021.02.002.

[28] S. Zhao, D. Yin, Y. Yu, S. Kang, D. Qin, L. Dong, $PM_{2.5}$ and O_3 pollution during 2015–2019 over 367 Chinese cities: Spatiotemporal variations, meteorological and topographical impacts, Environmental Pollution. 264 (2020) 114694. https://doi.org/10.1016/j.envpol.2020.114694.

[29] P. Sicard, Y.O. Khaniabadi, S. Leca, A. De Marco, Relationships between ozone and particles during air pollution episodes in arid continental climate, Atmospheric Pollution Research. 14(8) (2023) 101838. https://doi.org/10.1016/j.apr.2023.101838.

[30] Y. Zhang, J.J. West, R. Mathur, J. Xing, C. Hogrefe, S.J. Roselle, et al., Long-term trends in the ambient $PM_{2.5}$- and O_3-related mortality burdens in the United States under emission reductions from 1990 to 2010, Atmos. Chem. Phys. 18(20) (2018) 15003-15016. https://acp.copernicus.org/articles/18/15003/2018/.

[31] K. de Hoogh, J. Chen, J. Gulliver, B. Hoffmann, O. Hertel, M. Ketzel, et al., Spatial $PM_{2.5}$, NO_2, O_3 and BC models for Western Europe–Evaluation of spatiotemporal stability, Environment International. 120 (2018) 81-92. https://doi.org/10.1016/j.envint.2018.07.036.

[32] P. Sicard, E. Agathokleous, A. De Marco, E. Paoletti, V. Calatayud, Urban population exposure to air pollution in Europe over the last decades, Environmental Sciences Europe. 33(1) (2021) 28. https://doi.org/10.1186/s12302-020-00450-2.

[33] K. Li, D.J. Jacob, H. Liao, J. Zhu, V. Shah, L. Shen, et al., A two-pollutant strategy for improving ozone and particulate air quality in China, Nature Geoscience. 12(11) (2019) 906-910. https://doi.org/10.1038/s41561-019-0464-x.

[34] Y. Qu, T. Wang, C. Yuan, H. Wu, L. Gao, C. Huang, et al., The underlying mechanisms of $PM_{2.5}$ and O_3 synergistic pollution in East China: Photochemical and heterogeneous interactions, Science of The Total Environment. 873 (2023) 162434. https://doi.org/10.1016/j.scitotenv.2023.162434.

[35] P. Sicard, E. Agathokleous, S.C. Anenberg, A. De Marco, E. Paoletti, V. Calatayud, Trends in urban air pollution over the last two decades: A global perspective, Science of The Total Environment. 858 (2023) 160064. https://doi.org/10.1016/j.scitotenv.2022.160064.

[36] E. Agathokleous, Z. Feng, P. Sicard, Surge in nocturnal ozone pollution, Science. 382 (2023) 1131-1131. https://doi.org/10.1126/science.adm7628.

[37] F. Wang, W. Wang, Z. Wang, Z. Zhang, Y. Feng, A.G. Russell, et al., Drivers of PM(2.5)-O(3) co-pollution: from the perspective of reactive nitrogen conversion pathways in atmospheric nitrogen cycling, Sci Bull (Beijing). 67(18) (2022) 1833-1836. https://doi.org/10.1016/j.scib.2022.08.016.

[38] H. Dai, J. An, C. Huang, H. Wang, M. Zhou, L. Qiao, et al., Roadmap of coordinated control of $PM_{2.5}$ and ozone in Yangtze River Delta, Chinese Science Bulletin. 67(18) (2022) 2100-2112. https://doi.org/10.1360/TB-2021-0774.

[39] S. Faridi, M. Shamsipour, M. Krzyzanowski, N. Künzli, H. Amini, F. Azimi, et al., Long-term trends and health impact of $PM_{2.5}$ and O_3 in Tehran, Iran, 2006–2015, Environment International. 114 (2018) 37-49. https://doi.org/10.1016/j.envint.2018.02.026.

[40] J. Rentschler, N. Leonova, Global air pollution exposure and poverty, Nature Communications. 14(1) (2023) 4432. https://doi.org/10.1038/s41467-023-39797-4.

[41] A. Jbaily, X. Zhou, J. Liu, T.-H. Lee, L. Kamareddine, S. Verguet, et al., Air pollution exposure disparities across US population and income groups, Nature. 601(7892) (2022) 228-233. https://doi.org/10.1038/s41586-021-04190-y.

[42] A. Juginović, M. Vuković, I. Aranza, V. Biloš, Health impacts of air pollution exposure from 1990 to 2019 in 43 European countries, Scientific Reports. 11(1) (2021) 22516. https://doi.org/10.1038/s41598-021-01802-5.

[43] J. Lelieveld, J.S. Evans, M. Fnais, D. Giannadaki, A. Pozzer, The contribution of outdoor air pollution sources to premature mortality on a global scale, Nature. 525(7569) (2015) 367-371. https://doi.org/10.1038/nature15371.

[44] World Health Organization (WHO), WHO Global Air Quality Guidelines: ParticulateMatter ($PM_{2.5}$ and PM_{10}), Ozone, Nitrogen Dioxide, Sulfur Dioxide and Carbon Monoxide, World Health Organization, 2021. https://www.who.int/publications/i/item/9789240034228.

[45] W.-J. Guan, X.-Y. Zheng, K.F. Chung, N.-S. Zhong, Impact of air pollution on the burden of chronic respiratory diseases in China: time for urgent action, The Lancet. 388(10054) (2016) 1939-1951. https://doi.org/10.1016/S0140-6736(16)31597-5.

[46] C. Guerreiro, F. de Leeuw, V. Foltescu, Johannes, J. Aardenne, A. Luekewille, et al., Air Quality in Europe 2012 report, 2012. https://www.researchgate.net/publication/260600055_Air_Quality_in_Europe_2012_report.

[47] H.B. Mann, Nonparametric Tests Against Trend, Econometrica. 13 (1945) 245. http://www.jstor.org/stable/1907187.

[48] C. He, X. Niu, Z. Ye, Q. Wu, L. Liu, Y. Zhao, et al., Black carbon pollution in China from 2001 to 2019: Patterns, trends, and drivers, Environmental Pollution. 324 (2023) 121381. https://doi.org/10.1016/j.envpol.2023.121381.

[49] M. Strak, G. Weinmayr, S. Rodopoulou, J. Chen, K. de Hoogh, Z.J. Andersen, et al., Long term exposure to low level air pollution and mortality in eight European cohorts within the ELAPSE project: pooled analysis, Bmj. 374 (2021) n1904. https://doi.org/10.1136/bmj.n1904.

[50] B. Lu, Y. Hu, D. Yang, Y. Liu, L. Liao, Z. Yin, et al., GWmodelS: A software for geographically weighted models, SoftwareX. 21 (2023) 101291. https://doi.org/10.1016/j.softx.2022.101291.

[51] J. Ren, F. Guo, S. Xie, Diagnosing ozone–NOx–VOC sensitivity and revealing causes of ozone increases in China based on 2013–2021 satellite retrievals, Atmos. Chem. Phys. 22(22) (2022) 15035-15047. https://doi.org/10.5194/acp-22-15035-2022.

[52] Y. Wang, X. Yang, K. Wu, H. Mei, I. De Smedt, S. Wang, et al., Long-term trends of ozone and precursors from 2013 to 2020 in a megacity (Chengdu), China: Evidence of changing emissions and chemistry, Atmospheric Research. 278 (2022) 106309. https://doi.org/10.1016/j.atmosres.2022.106309.

[53] L. Zhu, M. Liu, J. Song, Spatiotemporal variations and influent factors of tropospheric ozone

concentration over China based on OMI data, Atmosphere. 13(2) (2022) 253. https://doi.org/10.3390/atmos13020253.

[54] Z. Yang, X. Yang, C. Xu, Q. Wang, The effect of meteorological features on pollution characteristics of $PM_{2.5}$ in the south area of Beijing, China, Atmosphere. 14(12) (2023) 1753. https://doi.org/10.3390/atmos14121753.

[55] M. Huo, K. Yamashita, F. Chen, K. Sato, Spatial-temporal variation in health impact attributable to $PM_{2.5}$ and ozone pollution in the Beijing metropolitan region of China, Atmosphere. 13(11) (2022) 1813. https://doi.org/10.3390/atmos13111813.

[56] L. Zhang, N. Zhao, W. Zhang, J.P. Wilson, Changes in long-term $PM_{2.5}$ pollution in the urban and suburban areas of China's three largest urban agglomerations from 2000 to 2020, Remote Sensing. 14(7) (2022) 1716. https://doi.org/10.3390/rs14071716.

[57] Y. Ma, Y. Zhang, W. Wang, P. Qin, H. Li, H. Jiao, et al., Estimation of health risk and economic loss attributable to $PM_{2.5}$ and O_3 pollution in Jilin Province, China, Scientific Reports. 13(1) (2023) 17717. https://doi.org/10.1038/s41598-023-45062-x.

[58] C. Zhu, C. Zhu, M. Qiu, Y. Gai, R. Li, L. Li, et al., Health burden and driving force changes due to exposure to $PM_{2.5}$ and O_3 from 2014 to 2060 in a typical industrial province, China, Atmosphere. 14(11) (2023) 1672. https://doi.org/10.3390/atmos14111672.

[59] X. Zhang, X. Xiao, F. Wang, G. Brasseur, S. Chen, J. Wang, et al., Observed sensitivities of $PM_{2.5}$ and O_3 extremes to meteorological conditions in China and implications for the future, Environment International. 168 (2022) 107428. https://doi.org/10.1016/j.envint.2022.107428.

[60] T. Liu, X. Wang, J. Hu, Q. Wang, J. An, K. Gong, et al., Driving forces of changes in air quality during the COVID-19 lockdown period in the Yangtze River Delta Region, China, Environmental Science & Technology Letters. 7(11) (2020) 779-786. https://doi.org/10.1021/acs.estlett.0c00511.

[61] Y. Wang, S. Zhu, J. Ma, J. Shen, P. Wang, P. Wang, et al., Enhanced atmospheric oxidation capacity and associated ozone increases during COVID-19 lockdown in the Yangtze River Delta, Science of The Total Environment. 768 (2021) 144796. https://doi.org/10.1016/j.scitotenv.2020.144796.

[62] T. Le, Y. Wang, L. Liu, J. Yang, Y.L. Yung, G. Li, et al., Unexpected air pollution with marked emission reductions during the COVID-19 outbreak in China, Science. 369(6504) (2020) 702-

706. https://doi.org/10.1126/science.abb7431.
[63] Y. Chen, G. Beig, S. Archer-Nicholls, W. Drysdale, W.J.F. Acton, D. Lowe, et al., Avoiding high ozone pollution in Delhi, India, Faraday Discussions. 226(0) (2021) 502-514. https://doi.org/10.1039/D0FD00079E.
[64] A. Pandey, M. Brauer, M.L. Cropper, K. Balakrishnan, P. Mathur, S. Dey, et al., Health and economic impact of air pollution in the states of India: the Global Burden of Disease Study 2019, The Lancet Planetary Health. 5(1) (2021) e25-e38. https://doi.org/10.1016/S2542-5196(20)30298-9.
[65] S. Muhammad, Y. Pan, M.H. Agha, M. Umar, S. Chen, Industrial structure, energy intensity and environmental efficiency across developed and developing economies: The intermediary role of primary, secondary and tertiary industry, Energy. 247 (2022) 123576. https://doi.org/10.1016/j.energy.2022.123576.
[66] M. Sahoo, N. Sethi, The dynamic impact of urbanization, structural transformation, and technological innovation on ecological footprint and $PM_{2.5}$: evidence from newly industrialized countries, Environment, Development and Sustainability. 24(3) (2022) 4244-4277. https://doi.org/10.1007/s10668-021-01614-7.
[67] J. Chen, C. Zhou, S. Wang, S. Li, Impacts of energy consumption structure, energy intensity, economic growth, urbanization on $PM_{2.5}$ concentrations in countries globally, Applied Energy. 230 (2018) 94-105. https://doi.org/10.1016/j.apenergy.2018.08.089.
[68] R. Zhu, Z. Tang, X. Chen, X. Liu, Z. Jiang, Rapid O_3 assimilations – Part 2: Tropospheric O_3 changes accompanied by declining NOx emissions in the USA and Europe in 2005–2020, Atmos. Chem. Phys. 23(17) (2023) 9745-9763. https://doi.org/10.5194/acp-23-9745-2023.
[69] J.L. Schnell, M.J. Prather, B. Josse, V. Naik, L.W. Horowitz, G. Zeng, et al., Effect of climate change on surface ozone over North America, Europe, and East Asia, Geophysical Research Letters. 43(7) (2016) 3509-3518. https://doi.org/10.1002/2016GL068060.
[70] M.O. Nawaz, D.K. Henze, S.C. Anenberg, D.Y. Ahn, D.L. Goldberg, C.W. Tessum, et al., Sources of air pollution-related health impacts and benefits of radially applied transportation policies in 14 US cities, Frontiers in Sustainable Cities. 5 (2023). https://doi.org/10.3389/frsc.2023.1102493.
[71] X. Querol, N. Pérez, C. Reche, M. Ealo, A. Ripoll, J. Tur, et al., African dust and air quality

over Spain: Is it only dust that matters?, Science of The Total Environment. 686 (2019) 737-752. https://doi.org/10.1016/j.scitotenv.2019.05.349.

[72] Y. Wang, W. Gao, S. Wang, T. Song, Z. Gong, D. Ji, et al., Contrasting trends of $PM_{2.5}$ and surface-ozone concentrations in China from 2013 to 2017, National Science Review. 7(8) (2020) 1331-1339. https://doi.org/10.1093/nsr/nwaa032.

[73] C.J. Lee, R.V. Martin, D.K. Henze, M. Brauer, A. Cohen, A.V. Donkelaar, Response of global particulate-matter-related mortality to changes in local precursor emissions, Environ Sci Technol. 49(7) (2015) 4335-4344. https://doi.org/10.1021/acs.est.5b00873.

[74] H. Zhang, T. Luo, Y. Chen, K. Liu, H. Li, E. Pensa, et al., Highly Efficient Decomposition of Perfluorocarbons for over 1000 Hours via Active Site Regeneration, Angewandte Chemie International Edition. 62 (2023) e202305651. https://doi.org/10.1002/anie.202305651.

[75] Y. Chen, W. Qu, T. Luo, H. Zhang, J. Fu, H. Li, et al., Promoting C–F bond activation via proton donor for CF4 decomposition, Proceedings of the National Academy of Sciences. 120 (2023) e2312480120. https://doi.org/10.1073/pnas.2312480120.

[76] S. Zhao, T. Feng, X. Tie, X. Long, G. Li, J. Cao, et al., Impact of Climate Change on Siberian High and Wintertime Air Pollution in China in Past Two Decades, Earth's Future. 6 (2018) 118-133. https://doi.org/10.1002/2017EF000682.

[77] X. Sun, K. Wang, B. Li, Z. Zong, X. Shi, L. Ma, et al., Exploring the cause of $PM_{2.5}$ pollution episodes in a cold metropolis in China, Journal of Cleaner Production. 256 (2020) 120275. https://doi.org/10.1016/j.jclepro.2020.120275.

[78] J. Dong, P. Liu, H. Song, D. Yang, J. Yang, G. Song, et al., Effects of anthropogenic precursor emissions and meteorological conditions on $PM_{2.5}$ concentrations over the “2+26” cities of northern China, Environmental Pollution. 315 (2022) 120392. https://doi.org/10.1016/j.envpol.2022.120392.

[79] C. Deng, C. Qin, Z. Li, K. Li, Spatiotemporal variations of $PM_{2.5}$ pollution and its dynamic relationships with meteorological conditions in Beijing-Tianjin-Hebei region, Chemosphere. 301 (2022) 134640. https://doi.org/10.1016/j.chemosphere.2022.134640.

[80] S. Gong, L. Zhang, C. Liu, S. Lu, W. Pan, Y. Zhang, Multi-scale analysis of the impacts of meteorology and emissions on $PM_{2.5}$ and O_3 trends at various regions in China from 2013 to 2020 2. Key weather elements and emissions, Science of The Total Environment. 824 (2022)

153847. https://doi.org/10.1016/j.scitotenv.2022.153847.

[81] Z. Lan, B. Zhang, X. Huang, Q. Zhu, J. Yuan, L. Zeng, et al., Source apportionment of $PM_{2.5}$ light extinction in an urban atmosphere in China, Journal of Environmental Sciences. 63 (2018) 277-284. https://doi.org/10.1016/j.jes.2017.07.016.

[82] C. Li, P. Chen, S. Kang, F. Yan, Z. Hu, B. Qu, et al., Concentrations and light absorption characteristics of carbonaceous aerosol in $PM_{2.5}$ and PM10 of Lhasa city, the Tibetan Plateau, Atmospheric Environment. 127 (2016) 340-346. https://doi.org/10.1016/j.atmosenv.2015.12.059.

[83] C.Y. Chan, L.Y. Chan, Effect of meteorology and air pollutant transport on ozone episodes at a subtropical coastal Asian city, Hong Kong, Journal of Geophysical Research: Atmospheres. 105 (2000) 20707-20724. https://doi.org/10.1029/2000JD900140.

[84] R.K. Yadav, H. Gadhavi, A. Arora, K.K. Mohbey, S. Kumar, S. Lal, et al., Relation between $PM_{2.5}$ and O_3 over Different Urban Environmental Regimes in India, Urban Science. 7 (2023) 9. https://doi.org/10.3390/urbansci7010009.

[85] A. Sharma, T.K. Mandal, S.K. Sharma, D.K. Shukla, S. Singh, Relationships of surface ozone with its precursors, particulate matter and meteorology over Delhi, Journal of Atmospheric Chemistry. 74 (2017) 451-474. 10.1007/s10874-016-9351-7.

[86] S.H. Bran, R. Srivastava, Investigation of $PM_{2.5}$ mass concentration over India using a regional climate model, Environmental Pollution. 224 (2017) 484-493. https://doi.org/10.1016/j.envpol.2017.02.030.

[87] H. Hata, K. Inoue, H. Yoshikado, Y. Genchi, K. Tsunemi, Impact of introducing net-zero carbon strategies on tropospheric ozone (O_3) and fine particulate matter ($PM_{2.5}$) concentrations in Japanese region in 2050, Science of The Total Environment. 891 (2023) 164442. https://doi.org/10.1016/j.scitotenv.2023.164442.

[88] M.J. Yeo, Y.P. Kim, Long-term trends and affecting factors in the concentrations of criteria air pollutants in South Korea, Journal of Environmental Management. 317 (2022) 115458. https://doi.org/10.1016/j.jenvman.2022.115458.

[89] P.A. Kassomenos, S. Vardoulakis, A. Chaloulakou, A.K. Paschalidou, G. Grivas, R. Borge, et al., Study of PM_{10} and $PM_{2.5}$ levels in three European cities: Analysis of intra and inter urban variations, Atmospheric Environment. 87 (2014) 153-163.

https://doi.org/10.1016/j.atmosenv.2014.01.004.

[90] P. Karamchandani, Y. Long, G. Pirovano, A. Balzarini, G. Yarwood, Source-sector contributions to European ozone and fine PM in 2010 using AQMEII modeling data, Atmos. Chem. Phys. 17 (2017) 5643-5664. https://doi.org/10.5194/acp-17-5643-2017.

[91] C. Fanizza, B. De Berardis, F. Ietto, M.E. Soggiu, R. Schirò, M. Inglessis, et al., Analysis of major pollutants and physico-chemical characteristics of $PM_{2.5}$ at an urban site in Rome, Science of The Total Environment. 616-617 (2018) 1457-1468. https://doi.org/10.1016/j.scitotenv.2017.10.168.

[92] J.J.P. Kuenen, A.J.H. Visschedijk, M. Jozwicka, H.A.C. Denier van der Gon, TNO-MACC_II emission inventory; a multi-year (2003–2009) consistent high-resolution European emission inventory for air quality modelling, Atmos. Chem. Phys. 14 (2014) 10963-10976. https://doi.org/10.5194/acp-14-10963-2014.

[93] B. Diao, L. Ding, J. Cheng, X. Fang, Impact of transboundary $PM_{2.5}$ pollution on health risks and economic compensation in China, Journal of Cleaner Production. 326 (2021) 129312. https://doi.org/10.1016/j.jclepro.2021.129312.

[94] L.K. Baxter, R.M. Duvall, J. Sacks, Examining the effects of air pollution composition on within region differences in $PM_{2.5}$ mortality risk estimates, Journal of Exposure Science & Environmental Epidemiology. 23 (2013) 457-465. https://doi.org/10.1038/jes.2012.114.

[95] Y.-S. Wang, L.-C. Chang, F.-J. Chang, Explore Regional $PM_{2.5}$ Features and Compositions Causing Health Effects in Taiwan, Environ Manage. 67 (2021) 176-191. https://doi.org/10.1007/s00267-020-01391-5.

[96] P. Masselot, F. Sera, R. Schneider, H. Kan, E. Lavigne, A. Tobias, et al., Differential Mortality Risks Associated With $PM_{2.5}$ Components: A Multi-Country, Multi-City Study, Epidemiology Publish Ahead of Print. (2021). https://doi.org/10.1097/EDE.0000000000001455.

[97] K.-J. Liao, E. Tagaris, S.L. Napelenok, K. Manomaiphiboon, J.-H. Woo, P. Amar, et al., Current and Future Linked Responses of Ozone and $PM_{2.5}$ to Emission Controls, Environmental Science & Technology. 42 (2008) 4670-4675. https://doi.org/10.1021/es7028685.

[98] I.B. Pollack, T.B. Ryerson, M. Trainer, J.A. Neuman, J.M. Roberts, D.D. Parrish, Trends in ozone, its precursors, and related secondary oxidation products in Los Angeles, California: A synthesis of measurements from 1960 to 2010, Journal of Geophysical Research: Atmospheres.

118 (2013) 5893-5911. https://doi.org/10.1002/jgrd.50472.

[99] C. Warneke, J.A. de Gouw, J.S. Holloway, J. Peischl, T.B. Ryerson, E. Atlas, et al., Multiyear trends in volatile organic compounds in Los Angeles, California: Five decades of decreasing emissions, Journal of Geophysical Research: Atmospheres. 117 (2012). https://doi.org/10.1029/2012JD017899.

[100] I. Stanimirova, D.Q. Rich, A.G. Russell, P.K. Hopke, Common and distinct pollution sources identified from ambient $PM_{2.5}$ concentrations in two sites of Los Angeles Basin from 2005 to 2019, Environmental Pollution. 340 (2024) 122817. https://doi.org/10.1016/j.envpol.2023.122817.

[101] I. Gutiérrez-Avila, H. Riojas-Rodriguez, E. Colicino, J. Rush, M. Tamayo-Ortiz, V. Borja-Aburto, et al., Short-term exposure to $PM_{2.5}$ and 1.5 million deaths: a time-stratified case-crossover analysis in the Mexico City Metropolitan Area, Environmental Health. 22 (2023). https://doi.org/10.1186/s12940-023-01024-4.

[102] J.S. Sakthi, M.P. Jonathan, G. Gnanachandrasamy, S.S. Morales-García, P.F. Rodriguez-Espinosa, D.C. Escobedo-Urias, et al., Atmospheric Changes and Ozone Increase in Mexico City During 2020: Recommended Remedial Measures, in: P. Li, V. Elumalai (Eds.) Recent Advances in Environmental Sustainability, Springer International Publishing, Cham. (2023), pp. 209-236. https://doi.org/10.1007/978-3-031-34783-2_11.

[103] R.A. Broome, J. Powell, M.E. Cope, G.G. Morgan, The mortality effect of $PM_{2.5}$ sources in the Greater Metropolitan Region of Sydney, Australia, Environment International. 137 (2020) 105429. https://doi.org/10.1016/j.envint.2019.105429.

[104] G. Ulpiani, G. Ranzi, M. Santamouris, Local synergies and antagonisms between meteorological factors and air pollution: A 15-year comprehensive study in the Sydney region, Science of The Total Environment. 788 (2021) 147783. https://doi.org/10.1016/j.scitotenv.2021.147783.

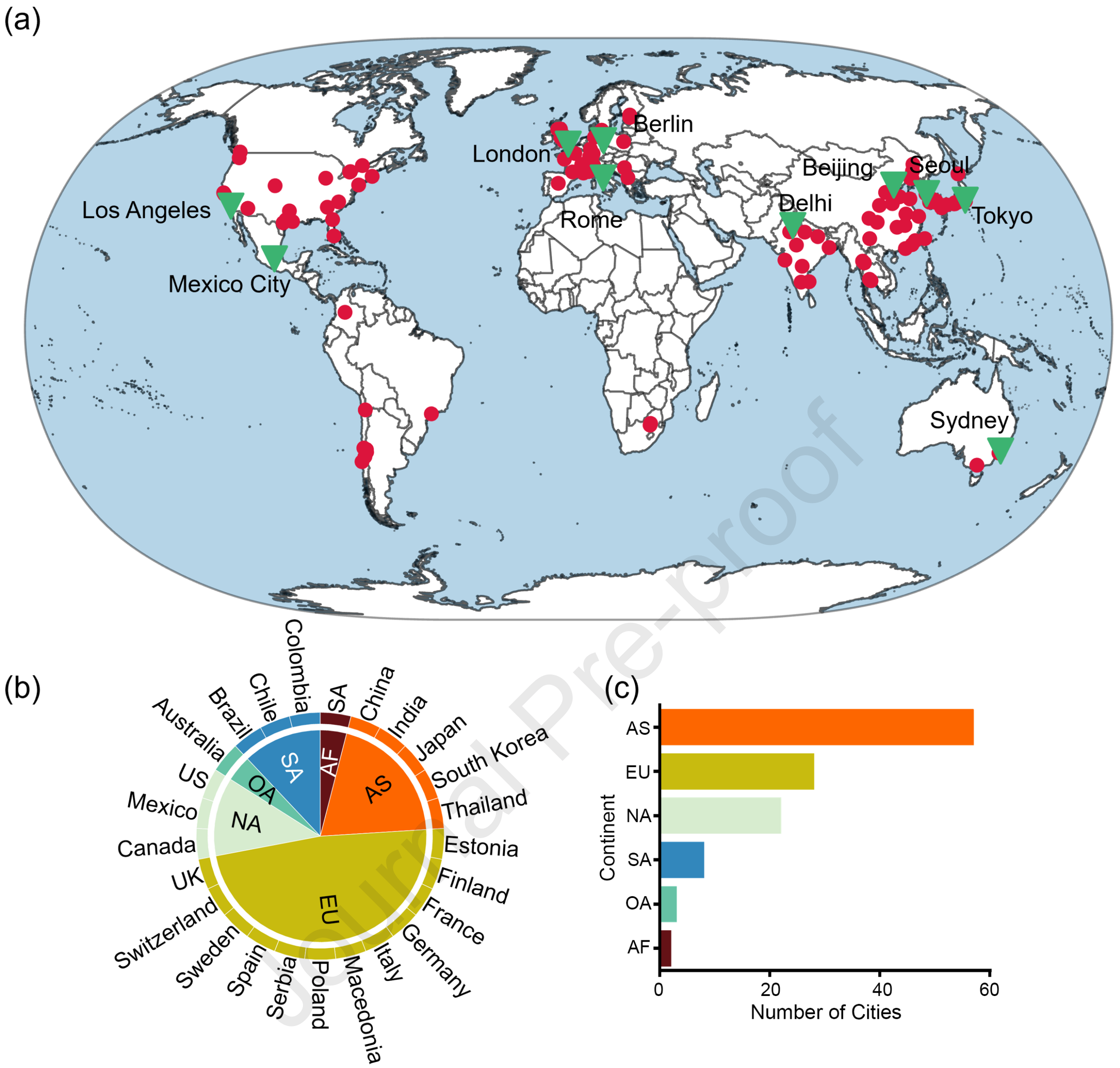
(a)
Berlin
London
Beijing
Seoul
Los Angeles
Delhi
Rome
Tokyo
Mexico City
Sydney
(b)
Colombia
SA
China
India
Japan
South Korea
Thailand
Estonia
Finland
France
Germany
Italy
Macedonia
Poland
Serbia
Spain
Sweden
Switzerland
UK
Canada
Mexico
US
Australia
Brazil
Chile
AF
AS
EU
NA
OA
(c)
AS
EU
NA
SA
OA
AF
Continent
0
20
40
60
Number of Cities

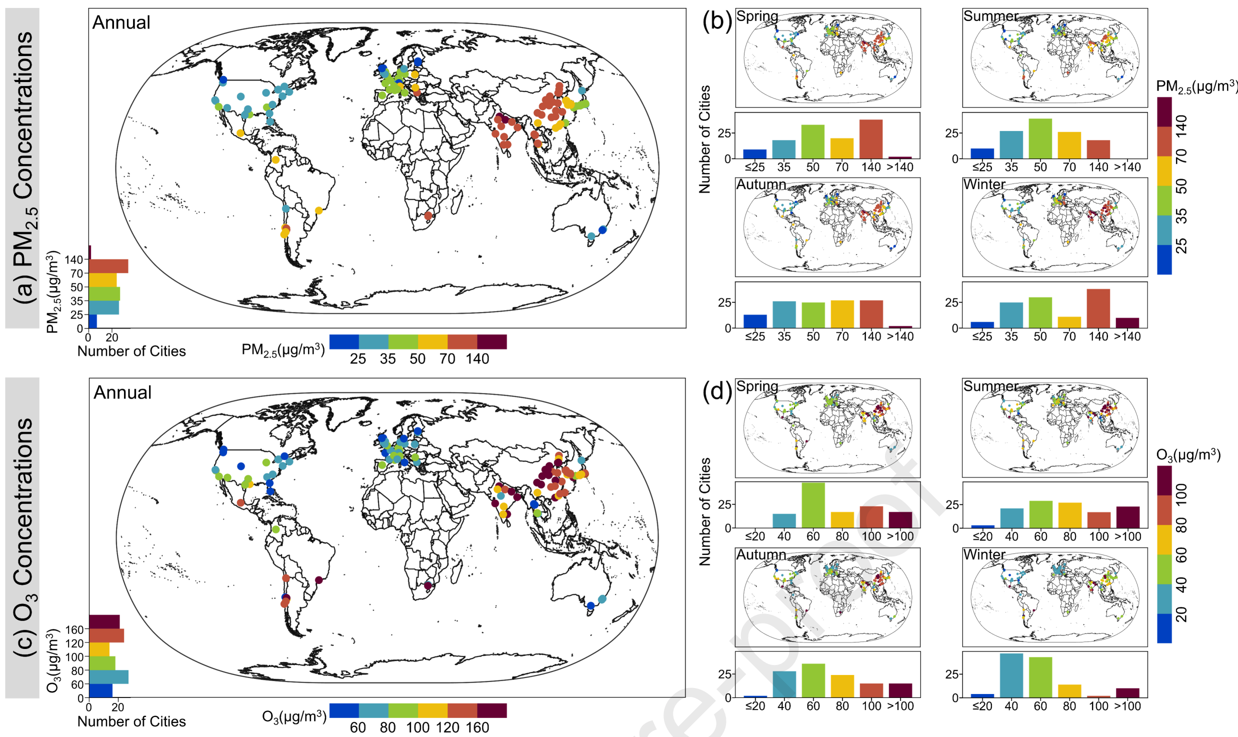
(a) PM2.5 Concentrations
Annual
PM2.5(μg/m3)
Number of Cities
25 35 50 70 140
(b)
Spring
Summer
Autumn
Winter
Number of Cities
≤25 35 50 70 140 >140
(c) O3 Concentrations
Annual
O3(μg/m3)
60 80 100 120 160
(d)
≤20 40 60 80 100 >100

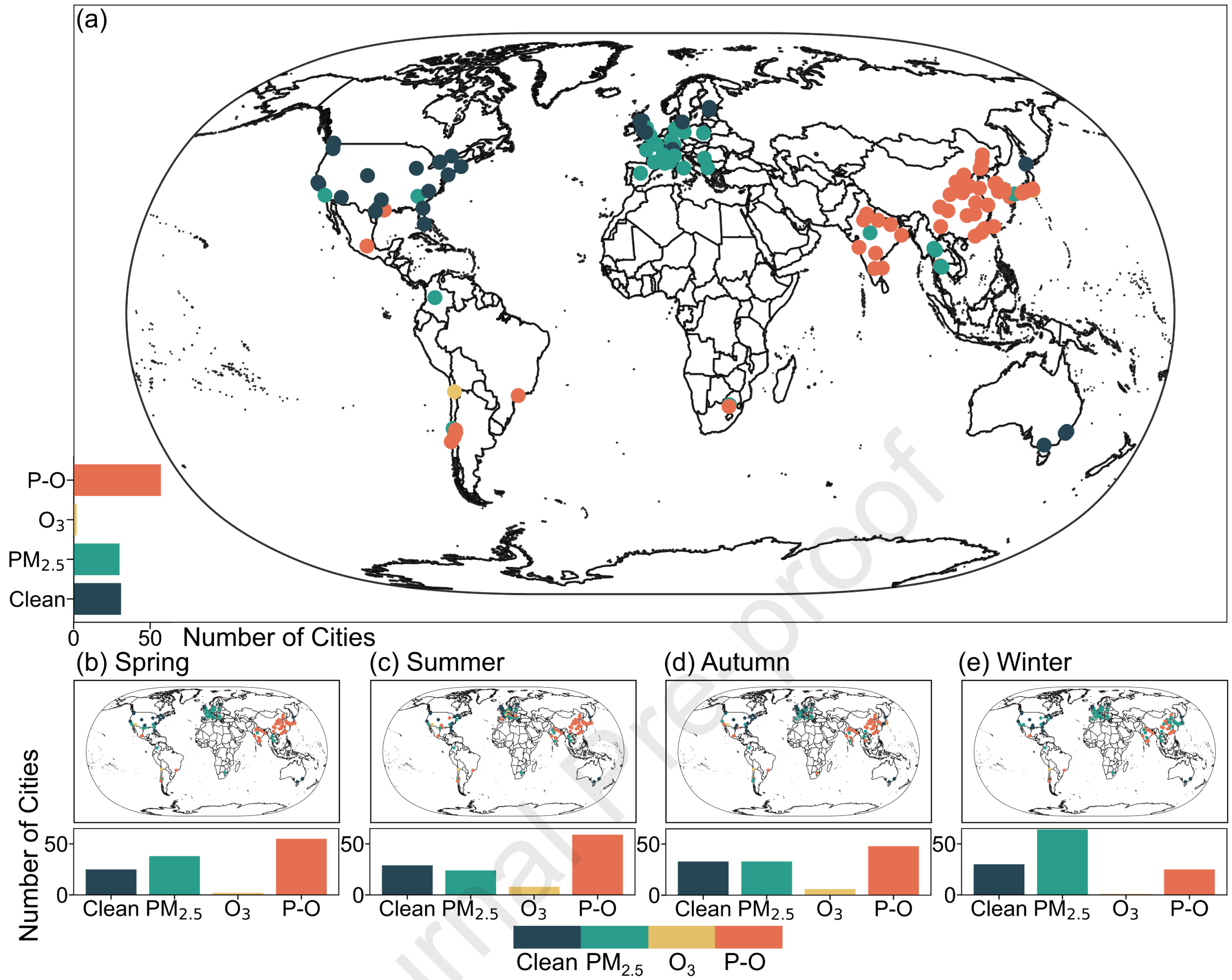
(a)
P-O
O_3
$PM_{2.5}$
Clean
0
50
Number of Cities
(b) Spring
(c) Summer
(d) Autumn
(e) Winter
Number of Cities
50
0
Clean
$PM_{2.5}$
O_3
P-O
Clean
$PM_{2.5}$
O_3
P-O

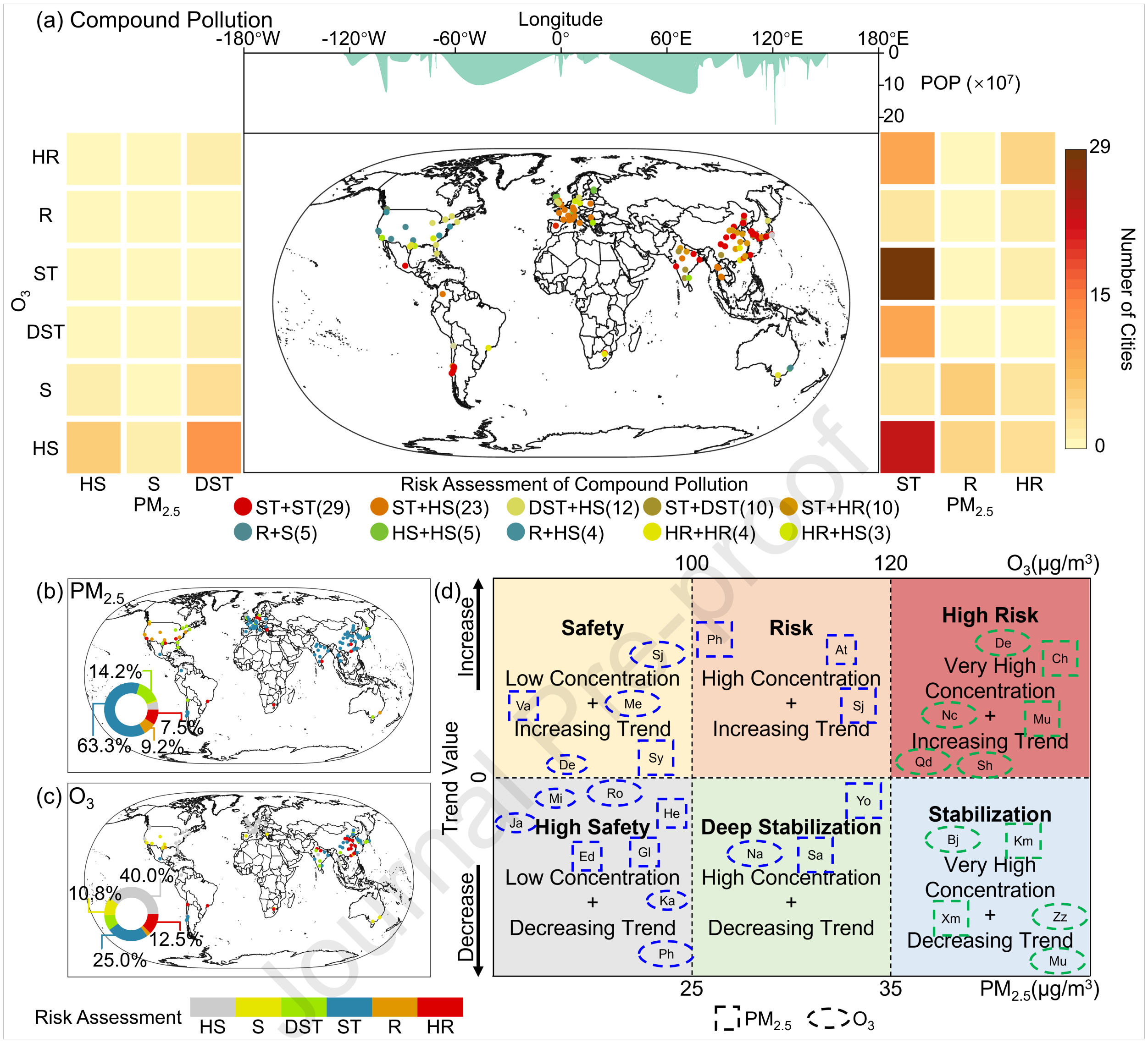
(a) Compound Pollution
Longitude
-180°W -120°W -60°W 0° 60°E 120°E 180°E
0 10 20 POP (×10^7)
HR R ST DST S HS
O3
HS S DST
PM2.5
ST R HR
PM2.5
29 15 0
Number of Cities
Risk Assessment of Compound Pollution
ST+ST(29) ST+HS(23) DST+HS(12) ST+DST(10) ST+HR(10)
R+S(5) HS+HS(5) R+HS(4) HR+HR(4) HR+HS(3)
(b) PM2.5
14.2% 7.5% 63.3% 9.2%
(c) O3
40.0% 10.8% 12.5% 25.0%
Risk Assessment
HS S DST ST R HR
(d)
100 120 O3(μg/m3)
Increase
Trend Value
0
Decrease
Safety
Low Concentration + Increasing Trend
Risk
High Concentration + Increasing Trend
High Risk
Very High Concentration + Increasing Trend
High Safety
Low Concentration + Decreasing Trend
Deep Stabilization
High Concentration + Decreasing Trend
Stabilization
Very High Concentration + Decreasing Trend
Sj Va Me De Sy Ph At Sj De Ch Nc Mu Qd Sh
Mi Ro Ja He Ed Gl Ka Ph Yo Na Sa Bj Km Xm Zz Mu
25 35 PM2.5(μg/m3)
PM2.5 O3

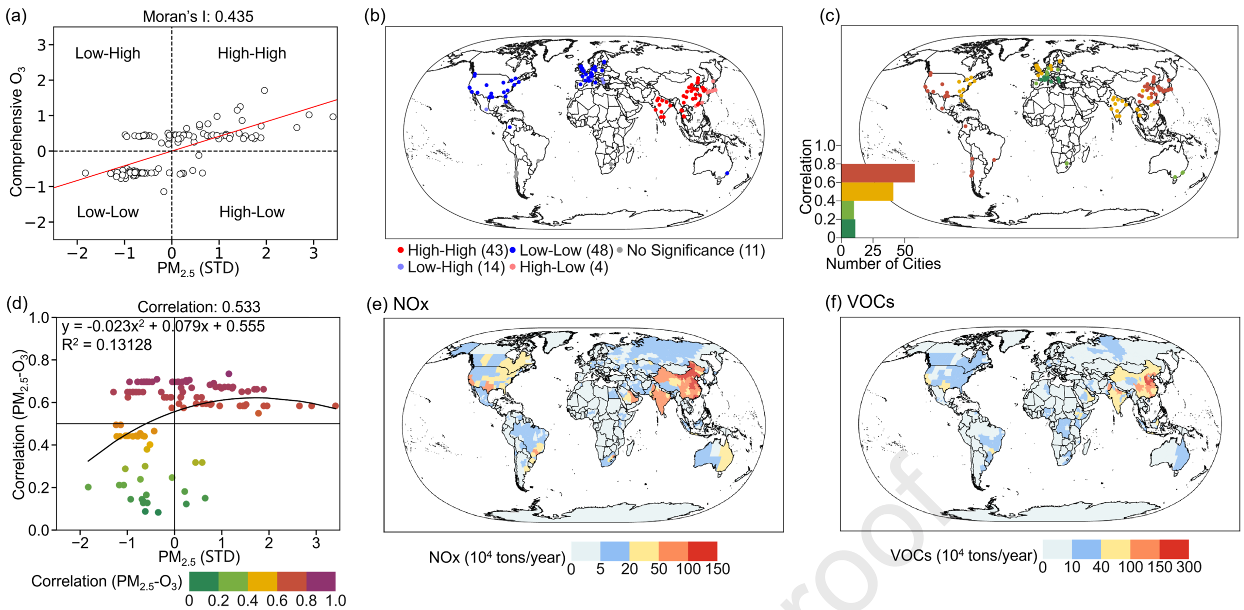
(a)
Moran's I: 0.435
Low-High
High-High
Low-Low
High-Low
Comprehensive O3
PM2.5 (STD)
(b)
High-High (43)
Low-Low (48)
No Significance (11)
Low-High (14)
High-Low (4)
(c)
Correlation
Number of Cities
(d)
Correlation: 0.533
y = -0.023x² + 0.079x + 0.555
R² = 0.13128
Correlation (PM2.5-O3)
PM2.5 (STD)
Correlation (PM2.5-O3)
0 0.2 0.4 0.6 0.8 1.0
(e) NOx
NOx (10⁴ tons/year)
0 5 20 50 100 150
(f) VOCs
VOCs (10⁴ tons/year)
0 10 40 100 150 300

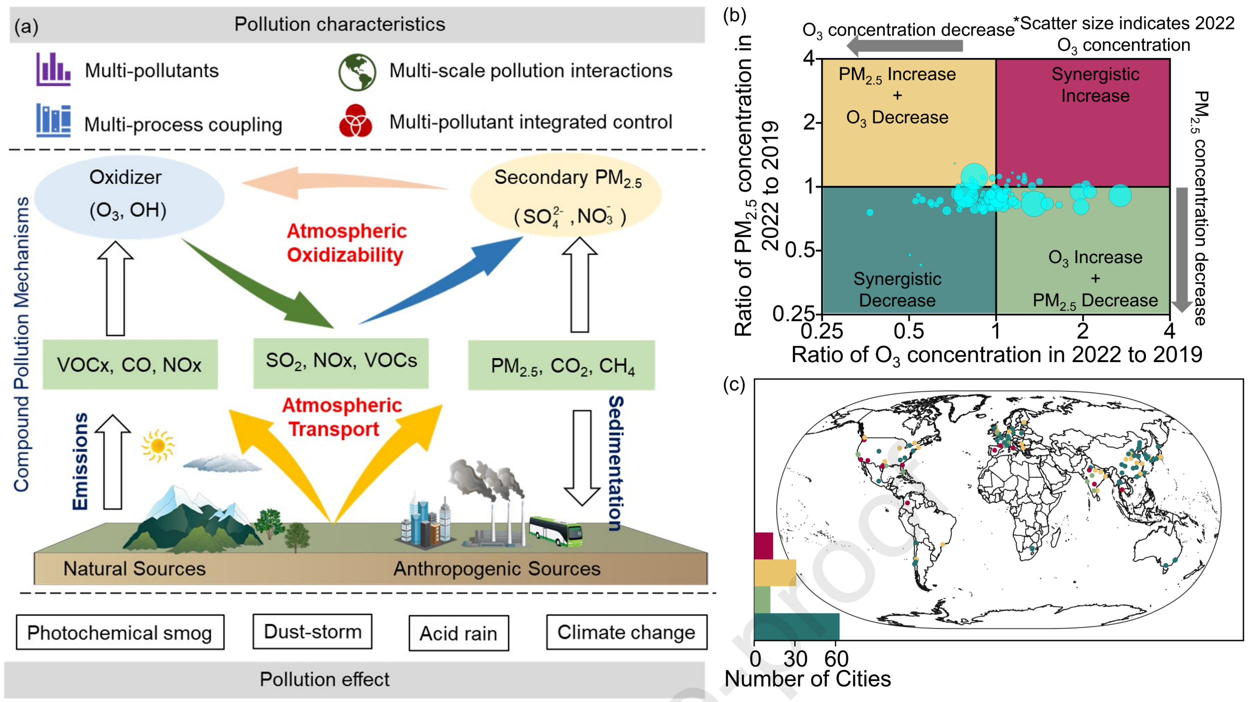
(a)
Pollution characteristics
Multi-pollutants
Multi-scale pollution interactions
Multi-process coupling
Multi-pollutant integrated control
Oxidizer
(O_3, OH)
Secondary $PM_{2.5}$
(SO_4^{2-}, NO_3^-)
Atmospheric Oxidizability
VOCx, CO, NOx
SO_2, NOx, VOCs
$PM_{2.5}$, CO_2, CH_4
Atmospheric Transport
Compound Pollution Mechanisms
Emissions
Sedimentation
Natural Sources
Anthropogenic Sources
Photochemical smog
Dust-storm
Acid rain
Climate change
Pollution effect
(b)
O_3 concentration decrease
*Scatter size indicates 2022 O_3 concentration
$PM_{2.5}$ Increase + O_3 Decrease
Synergistic Increase
Synergistic Decrease
O_3 Increase + $PM_{2.5}$ Decrease
$PM_{2.5}$ concentration decrease
Ratio of $PM_{2.5}$ concentration in 2022 to 2019
Ratio of O_3 concentration in 2022 to 2019
0.25
0.5
1
2
4
(c)
0
30
60
Number of Cities

Highlights

- 47.5% of assessed cities worldwide are exposed to compound $PM_{2.5}$-O_3 pollution.
- Cities in developing countries experience higher exposure risks than developed countries.
- Significant positive spatial correlations between $PM_{2.5}$ and O_3 concentrations are observed.
- 52.5% of cities worldwide have the potential for synergistic $PM_{2.5}$ and O_3 reductions.